MINISTRY OF AVIATION

AERONAUTICAL RESEARCH COUNCIL
REPORTS AND MEMORANDA

Aerodynamic Characteristics of Rectangular Wings of Small Aspect Ratio

By

I. J. CAMPBELL, C. F. BLANKS and D. A. LEAVER

LONDON: HER MAJESTY'S STATIONERY OFFICE

1960

TEN SHILLINGS NET

Aerodynamic Characteristics of Rectangular Wings of Small Aspect Ratio

By

I. J. Campbell, C. F. Blanks and D. A. Leaver

Reports and Memoranda No. 3142*

December, 1956

Summary.—The results of a programme of low-speed wind-tunnel measurements of the lift, drag and pitching moment on a number of model wings, each fitted with a full-span plain flap, and of a much more limited programme of hinge-moment measurements are presented. The wings differed from one another in profile but all were of rectangular plan-form and of aspect ratio 1·25. The flap chord was varied between 0·125 and 0·500 of the overall chord. Three of the profiles investigated were conventional in having zero trailing-edge thickness but the other three had large trailing-edge thickness, a feature thought to be of interest in connection with the design of torpedo fins.

Theoretical values of the lift slopes, hinge moments and positions of the centre of pressure were calculated from Lawrence's theory for thin rectangular wings of various aspect ratios in inviscid flow and the results are presented in tabular and graphical form. Predicted values, combining aspect-ratio effects with largely empirical allowances for thickness and boundary-layer effects, are checked against the measured values of the required aerodynamic characteristics of the ' conventional ' profiles and the agreement is fairly satisfactory. Although the aspect ratio was small, the induced drag associated with incidence and flap deflection was found to be well represented for all profiles by the usual expression derived from consideration of the elliptically loaded lifting line. A limited number of measurements suggested that the size of the gap between the control surface and the main part of the wing exercises little influence on the lift slopes, drag and c.p. positions if the gap width is less than 0·5 per cent of the overall chord.

---

1. *Introduction.*—The investigation reported here was undertaken to provide some data on the aerodynamic characteristics, particularly control characteristics, of small-aspect-ratio wings, needed in connection with studies of torpedo stability and control.

In the course of the investigation a programme of wind-tunnel measurements of lift, drag and pitching moment on six model wings, each fitted with a full-span plain flap, and a more limited programme of hinge-moment measurements were carried out. Attention was confined to the rectangular plan-form, which is of chief interest for our purposes, and, to limit the scope of the work further, the measurements were confined to only one aspect ratio, namely, 1·25. The profiles employed were all 5 per cent thick. Trailing-edge angle was one of the parameters varied. Also, since some earlier measurements[1] on a torpedo model had suggested that the control characteristics were improved, at the expense of a large but acceptable increase in drag, if streamlined fins were replaced by fins fitted with parallel-sided control surfaces of thickness equal to the maximum thickness of the fin, the trailing-edge thickness of the wing was varied in the present tests. A range of flap chords was covered and the influence of the size of the gap between the flap and the main part of the wing was examined.

Lawrence's theory[2] for low-aspect-ratio wings offers a convenient method of calculating the required aerodynamic characteristics for wings of zero thickness in inviscid flow but the experimental data available for checking the predictions for wings of small aspect ratio (near unity)

---

were considered inadequate. In this paper predicted values, combining aspect-ratio effects with allowances, largely empirical, for thickness and boundary-layer effects, are checked against experimental values for rectangular wings of aspect ratio 1·25.

2. *Lawrence's Small-Aspect-Ratio-Wing Theory.* — Lawrence's integral equation[2], which represents approximately the chordwise loading on a small-aspect-ratio wing, is as follows :

$$4k(\theta) = 2g(\theta) + g(0) + \beta(\theta) \int_0^\pi \frac{dg(\tau)}{d\tau} \frac{d\tau}{\cos \tau - \cos \theta} + \int_0^\pi \frac{dg(\tau)}{d\tau} H(\theta, \beta, \tau) \, d\tau \qquad .. \quad (1)$$

where

$$H(\theta, \beta, \tau) = \frac{\{(\cos \tau - \cos \theta)^2 + \beta^2(\theta)\}^{1/2} - \beta(\theta)}{\cos \tau - \cos \theta}$$

and $\beta(\theta) = $ the local semi-span, the semi-chord having been taken as unit length. In the present case of rectangular wings $\beta(\theta) = $ constant $= $ aspect ratio.

$$k(\theta) = \int_{-\beta}^{+\beta} w(\theta, y) \, (\beta^2 - y^2)^{1/2} dy = \frac{\pi}{2} \beta^2 w(\theta)$$

for a rectangular wing of zero twist.

The lift on the part of the wing forward of the chordwise position θ is proportional to $g(\theta)$ (for further details of the notation, *see* List of Symbols and Fig. 5a).

Lawrence expands $g(\theta)$ in the following series :

$$g(\theta) = (\pi - \theta)(A_0 + A_1) + \sum_{r=1}^{N-1} (A_{r-1} - A_{r+1}) \frac{\sin r\theta}{r} , \qquad .. \quad .. \quad .. \quad .. \quad (2)$$

where $A_{N-1} = A_N = 0$. The $(N - 1)$ coefficients, A_r, are to be determined by satisfying at $(N - 1)$ values of θ the following equation :

$$\frac{4}{\pi} k(\theta) = \{F_1(\theta) - F_0(\theta)\}A_0 + \sum_{r=1}^{N-2} \{F_{r+1}(\theta) - F_{r-1}(\theta)\}A_r , \qquad .. \quad .. \quad .. \quad .. \quad (3)$$

where

$$F_0(\theta) = \frac{2\theta}{\pi} + H_0(\theta, \beta) - 3 ,$$

$$F_r(\theta) = \frac{2 \sin r\theta}{\pi r} + \frac{\beta(\theta) \sin r\theta}{\sin \theta} + H_r(\theta, \beta) , \qquad (r = 1, 2, \ldots) ,$$

$$H_r(\theta, \beta) = \frac{1}{\pi} \int_0^\pi H(\theta, \beta, \tau) \cos r\tau \, d\tau .$$

Lawrence's theory has been used here to obtain theoretical values of a_2/a_1, b_1/a_1, b and x_c/c for rectangular wings of small aspect ratio. In carrying out the computations, equation (3) was satisfied at the six points along the profile where $\theta = 0$, $\pi/6$, $2\pi/6$, $3\pi/6$, $4\pi/6$, and $5\pi/6$. Since the value of $w(\theta)$ is introduced into the computation at only a limited number of points, there is inevitably in the case of profiles with a slope discontinuity some ambiguity about the position of the hinge line. In order to overcome this difficulty a continuous profile, of the form

$$z(\theta) = \sum_{k=0}^{4} \beta_k \cos k\theta, \qquad .. \quad .. \quad .. \quad .. \quad .. \quad .. \quad .. \quad .. \quad .. \quad (4)$$

was substituted for the discontinuous profile, the β_k being determined by the condition that the continuous profile should have the same lift, pitching moment and hinge moment at any angle of incidence (measured from the line joining the leading and trailing edge in both cases) when the aspect ratio is infinite. This technique must succeed for sufficiently large values of the aspect

2

ratio but it would not be surprising if it failed to give useful results at small values of the aspect ratio. At an aspect ratio of 1·25 the values of a_2/a_1 obtained with the substitution profile (4) lay on a smooth curve when plotted against E and the values obtained directly with the profile having a discontinuity in the shape were scattered about this curve. The values of x_c/c, calculated by the two methods, exhibited the same pattern. The use of the substitution profile does not arise in the calculation of b_1/a_1. In the calculation of b the scattered values were on the average about 10 per cent larger than the smoothed values obtained by use of the substitution profile. Even so it was considered worthwhile to use the substitution profile to obtain smoothed results when calculating b as well as a_2/a_1 and x_c/c for other values of the aspect ratio. Since the results, calculated by this method for an aspect ratio of 0·50, presented some small anomalies, we have not given results calculated in this way for values of the aspect ratio less than 1. Limiting values for the case when the aspect ratio becomes infinitesimally small can be obtained independently.

Lawrence shows that for a rectangular wing, in the limiting case where the aspect ratio tends to zero,

$$\lim_{\beta \to 0} g(\theta) = \int_{-\beta}^{+\beta} w(\theta, y) \, (\beta^2 - y^2)^{1/2} \, dy \, .$$

If the wing has zero twist, i.e., if $w(\theta, y)$ is independent of y,

$$\lim_{\beta \to 0} g(\theta) = \frac{\pi}{2} \beta^2 w(\theta) \, .$$

So, in the limiting case, the lift depends solely on the local angle of incidence at the trailing edge and, in the case of flat wings, the lift due to incidence is concentrated at the leading edge and the lift due to flap deflection is concentrated at the hinge. Thus, for flat rectangular wings, in the limiting case of zero aspect ratio, $a_2/a_1 = 1$, $b_1/a_1 = 0$ and $b = 0$ for all values of E and $x_c/c = 1 - E$.

Computed values of a_2/a_1, b_1/a_1, b and x_c/c for flat rectangular wings of various aspect ratios are presented in Tables 4, 5, 6 and 7 and also in Figs. 13, 15, 19 and 20.

3. *Description of the Experiments.*—Fig. 1 shows the wing profiles employed. All the profiles were symmetrical and had a thickness/chord ratio of 0·05. In each case the leading portion of the profile consisted of half an ellipse with a ratio of major to minor axes equal to 5 to 1. This was followed by a parallel portion and the trailing portion of the wing was formed by two circular arcs. a denotes the chordwise extent of the circular-arc trailing-edge portion and d the trailing-edge thickness. The specification of the profiles tested was as follows :

Profile	A	B	C	D	E	F
a/c	0·750	0·500	0·250	0·500	0·500	—
d/t	0	0	0	0·333	0·667	1·000 .

The chord and span of all models were 32 in. and 40 in. respectively. Each model was built up of a number of machined aluminium castings, held together internally by a number of short tongues. At the junction between the control surface and the main part of each model wing, angled tongues could be employed to hold the control surface at various fixed angles of deflection (*see* Fig. 2). In each case the gaps between the various sections of the model as well as between the control surface and the rest of the wing were sealed with thin cellulose tape. This was the arrangement employed for most of the measurements. The arrangement illustrated in Fig. 3 was used for the hinge-moment measurements and when a few measurements were made to explore the influence of the size of the gap, when unsealed, between the control surface and the main part of the wing.

The measurements were made in the 13 ft × 9 ft Wind Tunnel at the National Physical Laboratory. The method of suspending the models from the tunnel roof balance is illustrated in Fig. 4. An image strut was used to evaluate strut interference effects.

3

Wires of $0 \cdot 014$-in. diameter were glued to both surfaces at $0 \cdot 05c$ from the leading edge to fix the position of boundary-layer transition. Sufficient tests were made by the paraffin evaporation method to ensure that transition was taking place at the wire on both surfaces over the range of values of incidence and control-surface deflection employed during the experiments.

The measurements were made at a Reynolds number, based on chord, of $2 \cdot 6 \times 10^6$.

Corrections were made to the results to allow for wind-tunnel boundary constraint, support-strut interference effects, drag on the support struts and the rear suspension wire and drag on the transition wires.

The measured values of the most important coefficients are given in Tables 1, 2 and 3. Some typical sets of measurements are plotted in Figs. 6a to 11b and in Figs. 18a and 18b (for the notation *see* List of Symbols and Fig. 5b).

4. *Discussion of the Results.*—4.1. *The Variation of Lift Coefficient with Incidence.*—Values of $(a_{10})_T$, the theoretical lift-curve slope of a two-dimensional profile in incompressible potential flow, have been related to the thickness/chord ratio and the trailing-edge angle, ε_T, by Bryant, Halliday and Batson (*see* Fig. 5 of Ref. (3)). Collingbourne[4] has given empirical curves from which a_{10}, the lift slope of the two-dimensional profile allowing for boundary-layer effects, can be obtained. Collingbourne's relation at a Reynolds number of 6×10^6 between Δ, which denotes $(a_{10})_T - a_{10}$ and ε, the angle between lines cutting the profile on each surface at $0 \cdot 90c$ and $0 \cdot 99c$, and his relation between Δ and Reynolds number are reproduced in Figs. 12a and 12b. To deduce a_1, the lift-curve slope of the finite-aspect-ratio wing, Collingbourne suggests for unswept wings the relation

$$\frac{1}{a_1} = \frac{1}{a_{10}} + \frac{1}{\pi A}\left[1 + \frac{A}{2}\left\{\left(1 + \frac{4}{A^2}\right)^{1/2} - 1\right\}\right]. \qquad \qquad (5)$$

For profiles A, B and C at the Reynolds number of test ($2 \cdot 6 \times 10^6$) and for an aspect ratio of $1 \cdot 25$, the estimated and measured values of a_1 are compared in the accompanying Table. It will be seen that this method of estimating a_1 works well in the present cases. The value of a_1, derived by Lawrence's theory, making no allowance for thickness or boundary-layer effects is $1 \cdot 75$.

Profile	t/c	ε_T (deg)	ε (deg)	$(a_{10})_T$	$\Delta(6 \times 10^6)$	$\dfrac{\Delta(6 \times 10^6)}{\Delta(2 \cdot 6 \times 10^6)}$	$Re = 2 \cdot 6 \times 10^6$			
							Δ	a_{10}	Estimated a_1	Measured a_1
A	$0 \cdot 05$	$7 \cdot 6$	$7 \cdot 0$	$6 \cdot 53$	$0 \cdot 43$	$0 \cdot 79$	$0 \cdot 54$	$5 \cdot 99$	$1 \cdot 78$	$1 \cdot 85$
B	$0 \cdot 05$	$11 \cdot 5$	$10 \cdot 2$	$6 \cdot 54$	$0 \cdot 52$	$0 \cdot 79$	$0 \cdot 66$	$5 \cdot 88$	$1 \cdot 77$	$1 \cdot 80$
C	$0 \cdot 05$	$22 \cdot 8$	$17 \cdot 9$	$6 \cdot 55$	$0 \cdot 90$	$0 \cdot 79$	$1 \cdot 14$	$5 \cdot 41$	$1 \cdot 72$	$1 \cdot 75$

Comparing in Table 1 the values of a_1 for profiles D, E and F with those for profiles A, B and C, it can be seen how surprisingly little influence trailing-edge thickness has on the lift-curve slope.

4.2. *The Variation of Lift Coefficient with Flap Angle.*—Bryant, Halliday and Batson[3] have discussed in a comprehensive manner the factors governing the value of a_2 for two-dimensional aerofoils and they have given some curves, derived empirically, from which $a_{20}/(a_{20})_T$ can be estimated. Here a_{20} denotes the value of a_2 for a two-dimensional profile and $(a_{20})_T$ the theoretical value when no allowance is made for boundary-layer effects. Specifically in Fig. 17 of Ref. (3) $a_{20}/(a_{20})_T$ is plotted against E for various constant values of $a_{10}/(a_{10})_T$ and the authors suggest that these curves are independent of transition position and probably of Reynolds number : the values of $a_{20}/(a_{20})_T$ appropriate to profiles A, B and C have been obtained from this Figure by interpolation or extrapolation and are given in the attached Table. The values of

4

$(a_{20})_T$ were determined, using the values of $(a_{10})_T$ given in Section 4.1, on the assumption that $(a_{20}/a_{10})_T$ is independent of thickness and has the same value for profiles A, B and C as for thin flat plates. Hence the values of a_{20} and, using the estimated values of a_{10} given in Section 4.1, of a_{20}/a_{10} could be obtained.

According to lifting-line theory a_2/a_1 should be independent of aspect ratio. However, calculations based on Lawrence's theory show a progressive change in a_2/a_1 as the aspect ratio is decreased. The results of such calculations for rectangular wings of various aspect ratios and with various values of E are presented in Table 4 and in Fig. 13. In the attached Table, estimated values of a_2/a_1 for profiles A, B and C at aspect ratio 1·25 have been obtained simply by scaling up the values of a_{20}/a_{10} in proportion to the change of a_2/a_1 for a thin flat plate in inviscid flow when the aspect ratio is decreased from infinity to 1·25, $i.e.$,

$$\text{estimated value of } \frac{a_2}{a_1} = \frac{a_{20}}{a_{10}} \times$$

$$\times \frac{\text{Value of } a_2/a_1 \text{ for a thin flat plate of aspect ratio 1·25 in inviscid flow}}{\text{Value of } a_2/a_1 \text{ for a thin flat plate of infinite aspect ratio in inviscid flow}}.$$

Strictly speaking, of course, separate ' corrections ' for (low) aspect ratio and boundary-layer effects cannot be made and this is a crude procedure but there seems reasonable hope of success if it is applied to those quantities which according to lifting-line theory, are independent of aspect ratio. The procedure is to be justified by comparing the estimates, which it provides, with experimental results.

| Profile | E | $a_{10}/(a_{10})_T$ | $a_{20}/(a_{20})_T$ | a_{20}/a_{10} | Values of $(a_2/a_1)_t$ | | | $Re = 2·6 \times 10^6$ | |
					$A = \infty$	$A = 1·25$	Ratio	Estimated a_2/a_1	Measured a_2/a_1
A	0·250	0·917	0·933	0·619	0·609	0·724	1·19	0·737	0·643
B	0·125	0·899	0·807	0·394	0·441	0·556	1·26	0·496	0·467
	0·250	0·899	0·901	0·611	0·609	0·724	1·19	0·727	0·672
	0·375	0·899	0·933	0·756	0·728	0·825	1·13	0·854	0·783
	0·500	0·899	0·944	0·859	0·818	0·890	1·09	0·936	0·889
C	0·250	0·826	0·771	0·568	0·609	0·724	1·19	0·676	0·652

In fact, it will be seen from the Table that the agreement between estimated and measured values of a_2/a_1 is fairly good. In five of the six cases the estimated value is within 10 per cent of the measured value and in the remaining case (profile A) the discrepancy is less than 15 per cent. In every case the measured value of a_2/a_1 lies between the estimated value of a_2/a_1 and the estimated value of a_{20}/a_0. Estimated and measured values of a_2/a_1 for profile B are also compared in Fig. 14.

The measured values of a_2/a_1 for profiles D, E and F, listed in Table 1, are all somewhat greater than those for profiles A, B and C and in every case except one approach more closely the values predicted by Lawrence's theory. Indeed, in every case except one (profile F with $E = 0·250$) the measured values of a_2/a_1 for profiles D, E and F are within 5 per cent of the corresponding value of $(a_2/a_1)_t$ given by Lawrence's theory.

4.3. *Position of Centre of Pressure.*—Table 5 and Fig. 15 show how, according to Lawrence's theory, the position of the centre of pressure of the aerodynamic load due to flap deflection should vary with the ratio of flap chord to overall chord for rectangular wings of various aspect ratios. In each case, of course, the c.p. position, when E has the value unity, is the c.p. position of the aerodynamic load due to incidence. The accompanying Table shows how the measured values compare with the theoretical values for the particular cases of aspect ratio 1·25. It will

5

be seen that for profiles A and B the greatest discrepancy between the theoretical and measured c.p. position is less than $1\frac{1}{2}$ per cent of the overall chord while for profile C there are discrepancies of between 2 and 3 per cent of chord. Surprisingly the observed c.p. positions for profiles D,

Values of x_c/c : Wings of Rectangular Plan-form and Aspect Ratio 1·25

E	0·125	0·250	0·375	0·500	1·000
Theoretical value ..	0·677	0·597	0·516	0·434	0·183
Profile A		0·605			0·183
Profile B	0·663	0·590	0·520	0·427	0·176
Profile C		0·570			0·164
Profile D		0·598			0·186
Profile E		0·589			0·207
Profile F	0·676	0·584	0·523	0·436	0·206

E and F with large trailing-edge thickness are also in good agreement with theoretical expectation, the greatest discrepancy being less than 3 per cent of the chord. The measured results for profile E and the theoretical results for aspect ratio 1·25 are plotted in Fig. 16. It is clear that Lawrence's theory can be used confidently to predict c.p. position, at least for wings of rectangular plan-form.

4.4. *Drag.*—The values of the drag coefficient of each profile at zero incidence and with zero flap deflection are given in Table 1. The corresponding value of C_{D0} for a smooth flat plate at the same Reynolds number ($2\cdot6 \times 10^6$) and with the same transition position ($0\cdot05c$ downstream of the leading edge) is $0\cdot0073$. Naturally the profiles with finite trailing-edge thickness have a much larger drag than the profiles with zero trailing-edge thickness. Figs. 17a to 17f show that for all six profiles the induced drag associated with incidence or flap deflection is well represented, even for wings of such low aspect ratio, for all values of E by the expression $C_L^2/\pi A$, derived for an elliptically loaded lifting line. Some of the scatter is attributable to variations in profile drag with flap deflection.

4.5. *Gap Effects.*—All the results quoted previously were obtained with the gap between the control surface and the main part of the wing sealed. The effect of the size of the gap, when the gap is not sealed, was examined on profile F with a 25 per cent chord control surface only. The arrangement of the model of this purpose is illustrated in Fig. 3. The effects on a_1, a_2 and c.p. position are summarised in the accompanying Table :

Change in Value of Coefficients with Unsealed Gap   Profile F; $E = 0\cdot250$

Gap size (in.)	$\dfrac{\text{Gap}}{\text{Overall chord}}$ (per cent)	a_1	a_2	x_i/c	x_c/c
0·125	0·390	−0·04	0	−0·005	+0·014
0·250	0·781	−0·06	0	−0·004	+0·018

Unfortunately, before these measurements were made an accident in the tunnel resulted in bending of the support struts and, as no fresh determination of the support interference effect was made, the results have to be treated with caution. In fact, the values of a_1, a_2 and c.p. position were not quite the same with the present arrangement and a very small gap ($0\cdot010$ in.) as those obtained with the sealed-gap model arrangement (Fig. 2), used in the earlier measurements : it seemed reasonable to attribute the small discrepancies to changes in the support interference effect and to the small change in control-surface area. The differences quoted in the Table were obtained by comparison with the model arrangement of Fig. 3 with a gap of $0\cdot010$ in. ($0\cdot031$ per cent of overall chord) and it has been assumed that such a small gap is effectively a sealed gap.

It appears that the effects of the two gap sizes are small. a_1 is reduced by 2 or 3 per cent, a_2 is unaltered, the c.p. position of the aerodynamic load due to incidence is moved forward about $0 \cdot 5$ per cent of the overall chord and the c.p. position of the aerodynamic load due to flap deflection is moved back about $1 \cdot 5$ per cent of the overall chord.

It is more difficult to present a concise statement on the effect of gap size on drag. This is partly because the scatter of some of the results was rather too large to permit detailed analysis of rather small effects. Some correlation is naturally to be expected with C_L since this influences the flow through the gap. With $\alpha = 0$ and $\eta = 0$ $(C_L = 0)$, C_D was increased by about $0 \cdot 0003$ at gap sizes of $0 \cdot 125$ in. and $0 \cdot 250$ in. as compared with $0 \cdot 010$ in. With $\alpha = 6$ deg and $\eta = 6$ deg $(C_L = 0 \cdot 36)$, C_D was decreased by $0 \cdot 0011$ at a gap size of $0 \cdot 125$ in. and by $0 \cdot 0023$ at a gap size of $0 \cdot 250$ in. With $\alpha = 6$ deg and $\eta = -3$ deg $(C_L = 0 \cdot 14)$, C_D was the same at the three gap sizes of $0 \cdot 010$, $0 \cdot 125$ and $0 \cdot 250$ in.

For this case (profile F with $E = 0 \cdot 250$) at least, it seems clear that the size of the gap between the control surface and the main part of the wing exercises no very great influence on a_1, a_2, C_D or c.p. position, if the gap width is around $0 \cdot 5$ per cent or less of the overall chord.

4.6. *Hinge Moments.*—Hinge moments were measured only in two cases, namely, on profiles B and F, each fitted with a 25 per cent flap. The measured values in the case of profile B are plotted in Figs. 18a and 18b : the corresponding curves for profile F exhibit qualitatively the same features of non-linearity. The values of b_1 and b_2 for both profiles are given in Table 3. It will be observed that the values are considerably larger for profile F than for profile B.

Estimates of hinge-moment coefficients for a wing with profile B and of infinite aspect ratio have been made by the method proposed by Bryant, Halliday and Batson[3]. The values of the relevant quantities used in the estimation of b_{10}/a_0 were as follows :

$$E = 0 \cdot 250, \quad t/c = 0 \cdot 05, \quad \varepsilon_T = 11 \cdot 5 \text{ deg}, \quad a_{10}/(a_{10})_T = 0 \cdot 899, \quad (b_{10}/a_{10})_T = -0 \cdot 0806,$$

$$b_{10}/a_{10} = 0 \cdot 86, \quad (b_{10}/a_{10})_T = -0 \cdot 0693.$$

Since the relevant data in Ref. (3) relate only to values of E equal to $0 \cdot 20$ and $0 \cdot 40$, the value corresponding to an E of $0 \cdot 250$ was obtained by linear interpolation ; this seemed not too serious a risk since the two values given differed by only about 10 per cent. The values of further relevant quantities used in the estimation of b_0 were as follows :

$$(b_{10}/b_{20})_T = 0 \cdot 599, \quad (b_{20}/a_{10}) = (b_{20}/a_{10})_T \text{ in this particular instance,}$$

$$b_{20} = -0 \cdot 791, \quad b_0 = -0 \cdot 542.$$

A similar difficulty arose in the estimation of b_{20}/a_{10} to that which arose in the estimation of b_{10}/a_{10}.

According to lifting-line theory b_1/a_1 and b are independent of aspect ratio. Calculations based on Lawrence's theory, however, show a gradual change of both these quantities as the aspect ratio is decreased. The results of such calculations for rectangular wings of various aspect ratios and with various values of E are presented in Tables 6 and 7 and in Figs. 19 and 20. Estimated values of b_1/a_1 and of b were obtained by scaling up the values of b_{10}/a_0 and of b_0 in the following way :

$$\text{estimated value of } \frac{b_1}{a_1} \text{ (or } b) = \frac{b_{10}}{a_{10}} \text{ (or } b_0) \times$$

$$\times \frac{\text{Value of } b_1/a_1 \text{ (or } b) \text{ for a thin flat plate of aspect ratio } 1 \cdot 25 \text{ in inviscid flow}}{\text{Value of } b_1/a_1 \text{ (or } b) \text{ for a thin flat plate of infinite aspect ratio in inviscid flow}}.$$

As already noted in Section 4.2, this is a somewhat crude procedure.

The estimated and measured values for profile B are as follows :

	b_1/a_1	b
Estimated	$-0 \cdot 036$	$-0 \cdot 427$
Measured	$-0 \cdot 026$	$-0 \cdot 396$

7

The percentage discrepancy between the estimated and measured values of b_1/a_1 is rather large but both estimated and measured values are dubious : the main point is that b_1 is a relatively small and unimportant quantity. The percentage discrepancy between the estimated and measured values of b is about 8 per cent. Since b_1 is small, this implies that the estimate of b_2 is reasonably good. In fact the estimated and measured values of b_2 are respectively $-0\cdot473$ and $-0\cdot427$, a discrepancy of just over 10 per cent. In view of the non-linearity shown in Fig. 18b, accuracy of estimation of this order seems adequate.

4.7. *Effect of Finite Trailing-Edge Thickness.*—Earlier measurements[1] on a torpedo model suggested that, if streamlined fins of aspect ratio about 1 were replaced by fins fitted with parallel-sided control surfaces of thickness equal to the maximum thickness of the fin, then a_2 should be increased by between 50 and 60 per cent for values of E lying between $0\cdot10$ and $0\cdot25$. This expectation has not been fulfilled in the present measurements on fins in the absence of a model torpedo hull. As already discussed, it can be seen from Tables 1 and 2 that the values of a_1 for profiles B and F are about the same while the value of a_2 for profile F is larger than that for profile B only by amounts varying from 5 to 13 per cent for values of E between $0\cdot125$ and $0\cdot500$. The measurements on the torpedo model were made at a Reynolds number (based on fin chord) rather less than one-fifth of that of the present measurements. It may be that profiles B and F would have shown the expected difference at the lower Reynolds number. Alternatively the much larger value of a_2 obtained in the earlier tests with the parallel-sided as compared with the streamlined control surfaces may have been due to a difference in the interaction between control surface and hull. Not only was the expected increase in a_2 not realised in the present measurements but it was also found that the hinge moment on the control with the thick trailing edge was greatly increased.

5. *Summary and Conclusions.*—The results of a programme of wind-tunnel measurements of the lift, drag and pitching moment on a number of model wings, each fitted with a full-span plain flap, and of a much more limited programme of hinge-moment measurements have been presented. The wings differed from one another in profile but all were of rectangular plan-form and of aspect ratio $1\cdot25$. The flap chord was varied between $0\cdot125$ and $0\cdot500$ of the overall chord. Three of the profiles investigated were conventional in having zero trailing-edge thickness but the other three had large trailing-edge thickness, a feature thought to be of interest in connection with the design of torpedo fins.

Contrary to expectation the present measurements do not suggest any substantial advantage from fins with finite trailing-edge thickness as compared with the 'conventional' profiles. Finite trailing-edge thickness gives rise to larger hinge moments and, of course, to greatly increased drag.

Theoretical values of a_2/a_1, b_1/a_1, b and of the positions of the centres of pressure of the aerodynamic load due to incidence and flap deflection for thin flat rectangular wings of various aspect ratios in inviscid flow have been calculated and the results are presented in graphical and tabular form. The influence of thickness and boundary-layer effects on the two-dimensional characteristics of the profiles employed has been assessed from the best available (mainly empirical) data. The measure of agreement between the predicted values, obtained by combining thickness, boundary-layer and aspect-ratio effects and the measured values of a_1, a_2/a_1, b_1/a_1, b and of c.p. positions for the conventional profiles is fairly satisfactory. Although the aspect ratio was small, the induced drag associated with incidence and flap deflection was found to be well represented by the usual expression derived from consideration of the elliptically loaded lifting line. A limited number of measurements suggested that the size of the gap between the control surface and the main part of the wing exercises little influence on a_1, a_2, C_D or c.p. position if the gap width is less than $0\cdot5$ per cent of the overall chord.

8

LIST OF SYMBOLS

a		A geometrical parameter used in specifying profiles (*see* first paragraph of Section 3)
a_{10}	$=$	$\partial C_L / \partial \alpha$ for a two-dimensional profile
$(a_{10})_T$		Theoretical value of a_{10}, including thickness but not boundary-layer effects
a_1	$=$	$\partial C_L / \partial \alpha$ for a wing of finite aspect ratio
$(a_1)_t$		Theoretical value of a_1, no allowance being made for thickness or boundary-layer effects
a_{20}	$=$	$\partial C_L / \partial \eta$ for a two-dimensional profile
$(a_{20})_T$		Theoretical value of a_{20}, including thickness but not boundary-layer effects
a_2	$=$	$\partial C_L / \partial \eta$ for a wing of finite aspect ratio
$(a_2)_t$		Theoretical value of a_2, no allowance being made for thickness or boundary-layer effects
A		Aspect ratio
A_r		Coefficients defined by equation (3)
b_{10}	$=$	$\partial C_H / \partial \alpha$ for a two-dimensional profile
$(b_{10})_T$		Theoretical value of b_{10}, including thickness but not boundary-layer effects
b_1	$=$	$\partial C_H / \partial \alpha$ for a wing of finite aspect ratio
$(b_1)_t$		Theoretical value of b_1, no allowance being made for thickness or boundary-layer effects.
b_{20}	$=$	$\partial C_H / \partial \eta$ for a two-dimensional profile
$(b_{20})_T$		Theoretical value of b_{20}, including thickness but not boundary-layer effects
b_2	$=$	$\partial C_H / \partial \eta$ for a wing of finite aspect ratio
$(b_2)_t$		Theoretical value of b_2, no allowance being made for thickness or boundary-layer effects
b_0	$=$	$b_{20} - \dfrac{a_{20}}{a_0} b_{10}$
b	$=$	$b_2 - \dfrac{a_2}{a_1} b_1$
b_t	$=$	$(b_2)_t - \left(\dfrac{a_2}{a_1}\right)_t (b_1)_t$
c		Wing chord
C_D		Drag coefficient
C_{D0}		Value of C_D when α and η are both zero
C_H		Hinge-moment coefficient (based on control-surface area and control-surface chord)
C_L		Lift coefficient
C_m		Pitching-moment coefficient (referred to leading edge)
d		Trailing-edge thickness

9

E	Ratio of flap chord to overall chord
$F_r(\theta)$	Functions defined following equation (3)
$g(\theta)$	(Lift on part of wing forward of the chordwise position θ)$/2\rho U^2$
$H(\theta, \beta, \tau)$	Functions defined following equation (1)
$H_r(\theta, \beta)$	Functions defined following equation (3)
$k(\theta)$	Function defined following equation (1)
t	Maximum thickness of aerofoil
U	Free-stream velocity
$- w(\theta, y)$	Local inclination of aerofoil mean camber line to free-stream direction
x_i	Centre-of-pressure position for aerodynamic load due to incidence (*see* Fig. 5b)
x_c	Centre-of-pressure position for aerodynamic load due to flap deflection (*see* Fig. 5b)
y, z	Co-ordinates defined in Fig. 5a
α	Angle of incidence
$\beta(\theta)$	Local semi-span of wing
β	Semi-span of rectangular wing
β_k	Coefficients defined in equation (4)
$\Delta = (a_0)_T - a_0$	
$\varepsilon, \varepsilon_T$	Trailing-edge angles (*see* Section 4)
η	Flap deflection angle
θ	Angle specifying chordwise position (*see* Fig. 5a)
ρ	Fluid density

REFERENCES

No.	Author	Title, etc.
1	C. F. Blanks and D. A. Leaver	A.R.L. Report (Unpublished).
2	H. R. Lawrence..	The lift distribution on low-aspect-ratio wings at subsonic speeds. *J. Ae. Sci.* pp. 683 to 695. October, 1951.
3	L. W. Bryant, A. S. Halliday and A. S. Batson.	Two-dimensional control characteristics. R. & M. 2730. April, 1950.
4	J. R. Collingbourne	A.R.C. Paper (Unpublished).

TABLE 1

$(\eta = 0)$

Profile	a/c	d/t	a_1	x_i/c	C_{D0}
A	0·750	0	1·85	0·183	0·0077
B	0·500	0	1·80	0·176	0·0082
C	0·250	0	1·75	0·164	0·0083
D	0·500	0·333	1·83	0·186	0·0119
E	0·500	0·667	1·85	0·207	0·0205
F	—	1·000	1·86	0·206	0·0279

TABLE 2

$(\alpha = 0)$

Profile	a/c	d/t	E	a_2	a_2/a_1	x_c/c
A	0·750	0	0·250	1·19	0·643	0·605
B	0·500	0	0·125	0·84	0·467	0·663
B	0·500	0	0·250	1·21	0·672	0·590
B	0·500	0	0·375	1·41	0·783	0·520
B	0·500	0	0·500	1·60	0·889	0·427
C	0·250	0	0·250	1·14	0·652	0·570
D	0·500	0·333	0·250	1·27	0·694	0·598
E	0·500	0·667	0·250	1·32	0·714	0·589
F	—	1·000	0·125	0·95	0·510	0·676
F	—	1·000	0·250	1·32	0·710	0·584
F	—	1·000	0·375	1·50	0·806	0·523
F	—	1·000	0·500	1·69	0·908	0·436

TABLE 3

Profile	a/c	d/t	E	b_1	b_1/a_1	b_2	b
B	0·500	0	0·250	—0·046	—0·026	—0·427	—0·396
F	—	1·000	0·250	—0·136	—0·073	—0·617	—0·520

11

TABLE 4

Values of $(a_2/a_1)_t$ for Flat Wings of Rectangular Plan-form according to Lawrence's Theory

E	0·050	0·125	0·250	0·375	0·500	0·750	1·000
A = 0	1·000	1·000	1·000	1·000	1·000	1·000	1·000
1	0·401	0·584	0·751	0·847	0·904	0·965	1·000
2	0·343	0·511	0·679	0·788	0·863	0·955	1·000
4	0·311	0·473	0·642	0·756	0·839	0·948	1·000
∞	0·282	0·441	0·609	0·728	0·818	0·942	1·000

TABLE 5

Values of x_c/c for Flat Wings of Rectangular Plan-form according to Lawrence's Theory

E	0·050	0·125	0·250	0·375	0·500	0·750	1·000
A = 0	0·950	0·875	0·750	0·625	0·500	0·250	0
1	0·766	0·706	0·622	0·535	0·445	0·274	0·167
2	0·660	0·618	0·549	0·479	0·411	0·286	0·209
4	0·585	0·550	0·493	0·437	0·383	0·289	0·231
∞	0·483	0·459	0·420	0·382	0·347	0·287	0·250

TABLE 6

Values of $(b_1/a_1)_t$ for Flat Wings of Rectangular Plan-form according to Lawrence's Theory

E	0·05	0·125	0·250	0·375	0·500	0·750	1·000
A = 0	0	0	0	0	0	0	0
1	—0·0161	—0·0260	—0·0387	—0·0504	—0·0633	—0·0973	—0·1674
2	—0·0265	—0·0429	—0·0632	—0·0811	—0·0989	—0·1399	—0·2089
4	—0·0338	—0·0539	—0·0781	—0·0989	—0·1192	—0·1634	—0·2309
∞	—0·0379	—0·0618	—0·0900	—0·1140	—0·1366	—0·1838	—0·2500

TABLE 7

Values of $(b)_t$ for Flat Wings of Rectangular Plan-form according to Lawrence's Theory

E	0·05	0·125	0·250	0·375	0·500	0·750	1·000
A = 0	0	0	0	0	0	0	0
1	—0·714	—0·600	—0·442	—0·320	—0·223	—0·082	0
2	—0·755	—0·659	—0·517	—0·396	—0·289	—0·114	0
4	—0·777	—0·692	—0·557	—0·436	—0·324	—0·132	0
∞	—0·798	—0·723	—0·599	—0·479	—0·363	—0·150	0
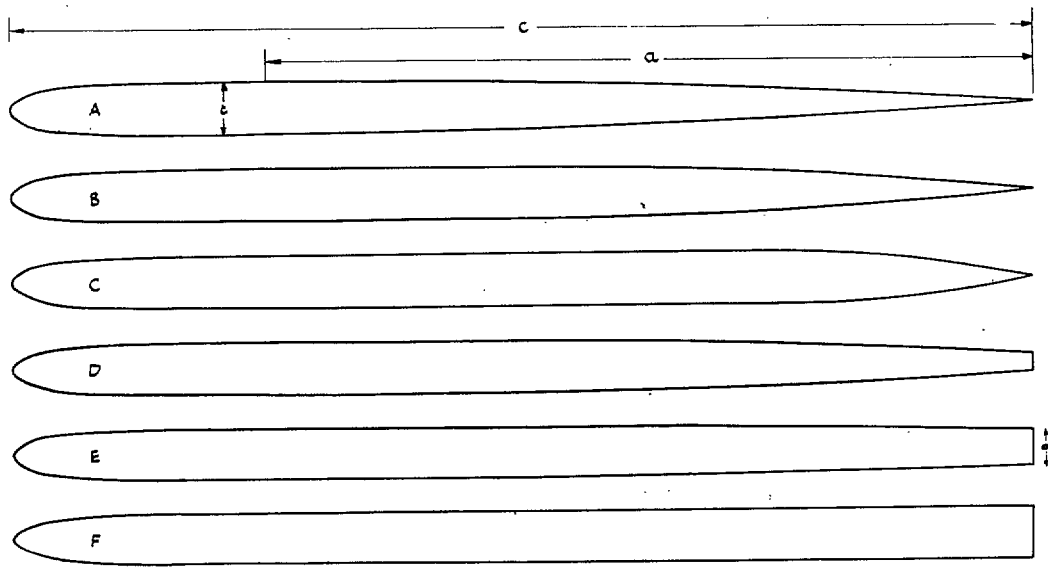
FIG. 1. Profiles.
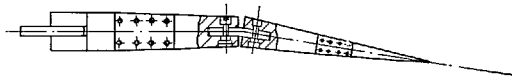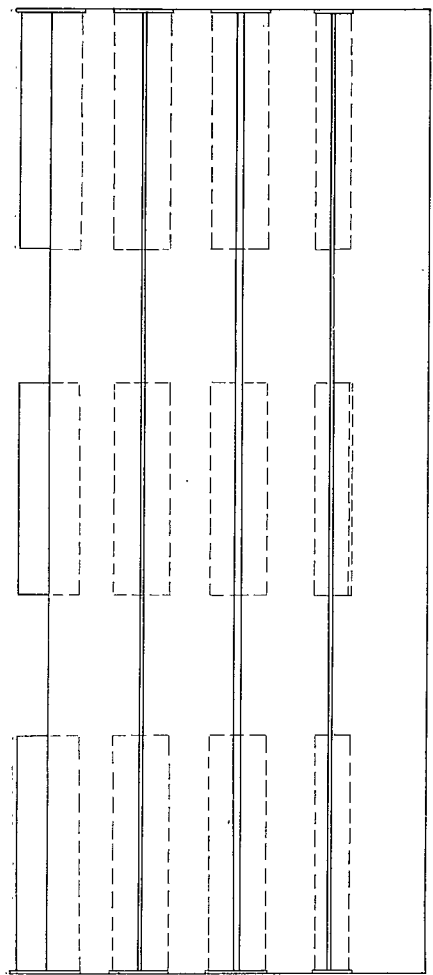
FIG. 2.   Fixed-hinge model.—9-deg
angle illustrated.

FLOW
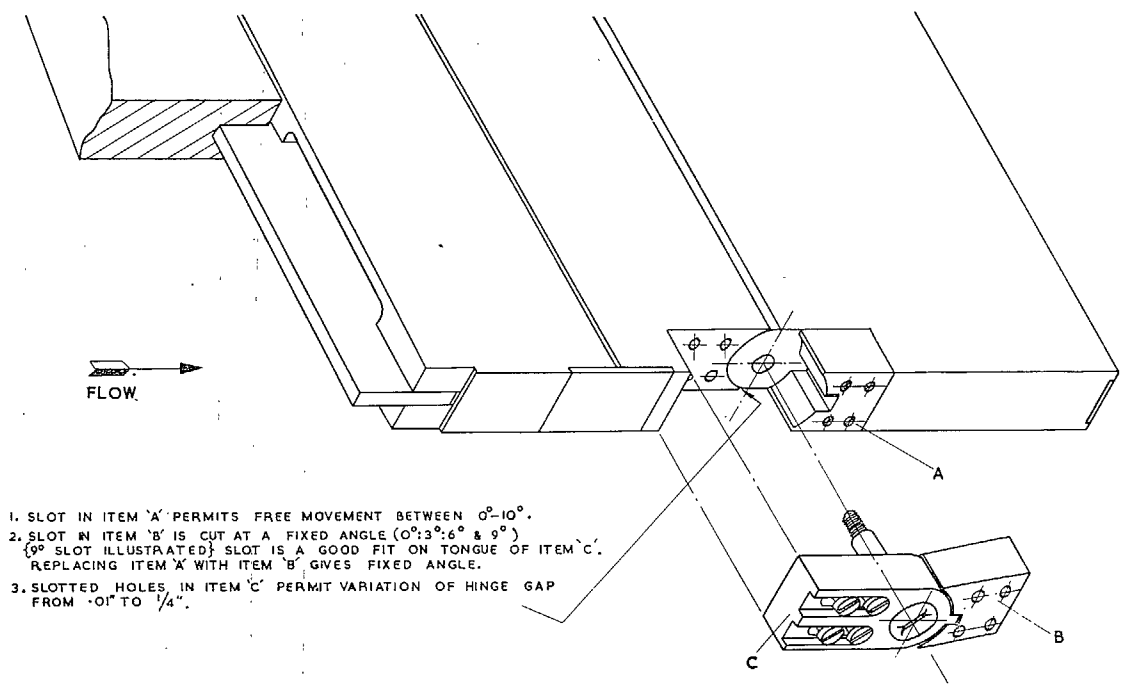
1. SLOT IN ITEM 'A' PERMITS FREE MOVEMENT BETWEEN 0°-10°.
2. SLOT IN ITEM 'B' IS CUT AT A FIXED ANGLE (0°:3°:6° & 9°)
   {9° SLOT ILLUSTRATED} SLOT IS A GOOD FIT ON TONGUE OF ITEM 'C'.
   REPLACING ITEM 'A' WITH ITEM 'B' GIVES FIXED ANGLE.
3. SLOTTED HOLES IN ITEM 'C' PERMIT VARIATION OF HINGE GAP
   FROM ·01" TO 1/4".

FIG. 3.   Scrap view of freely hinged joint.
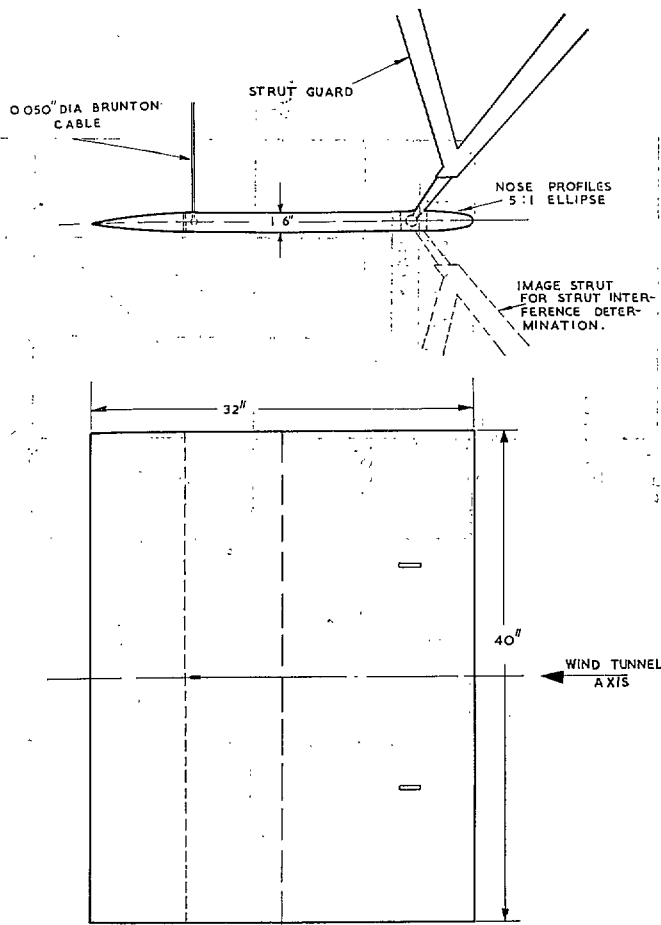
FIG. 4. General arrangement of
wind-tunnel model.
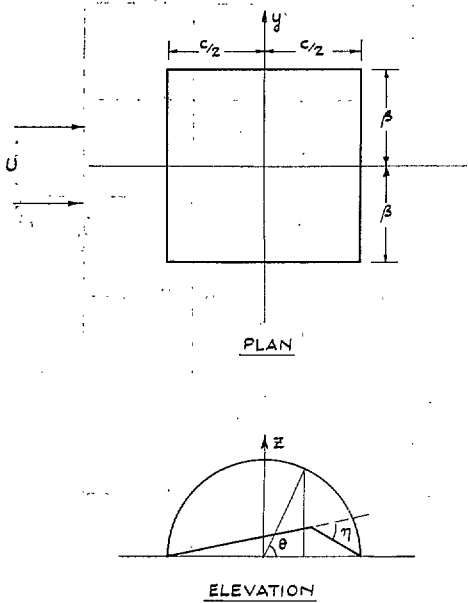
FIG. 5a. Notation.
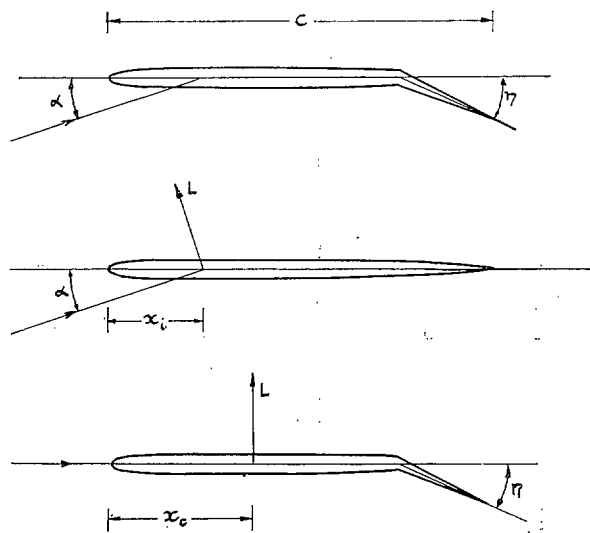
x_i DEFINES CENTRE OF PRESSURE OF AERODYNAMIC
LOAD DUE TO INCIDENCE

x_c DEFINES CENTRE OF PRESSURE OF AERODYNAMIC LOAD
DUE TO FLAP DEFLECTION.

FIG. 5b. Notation.
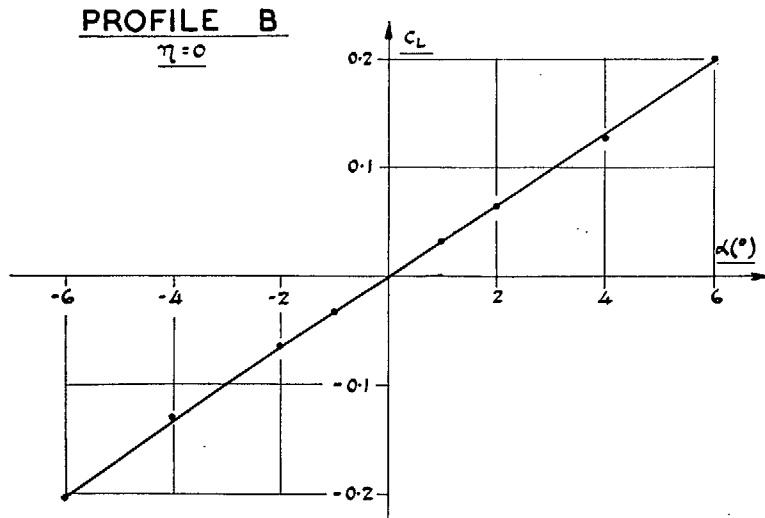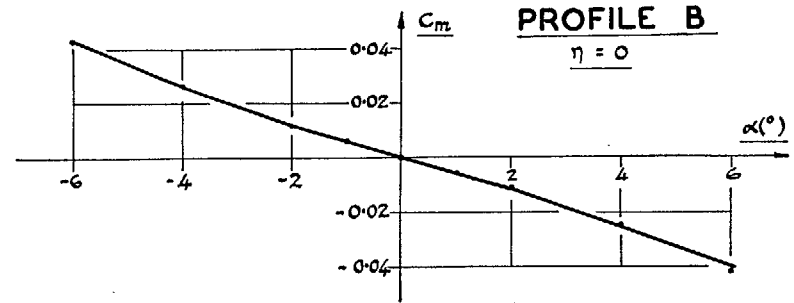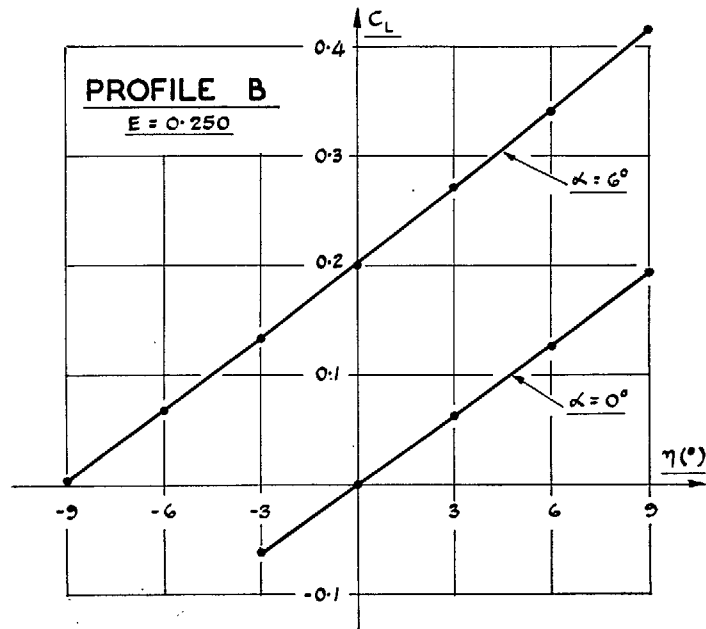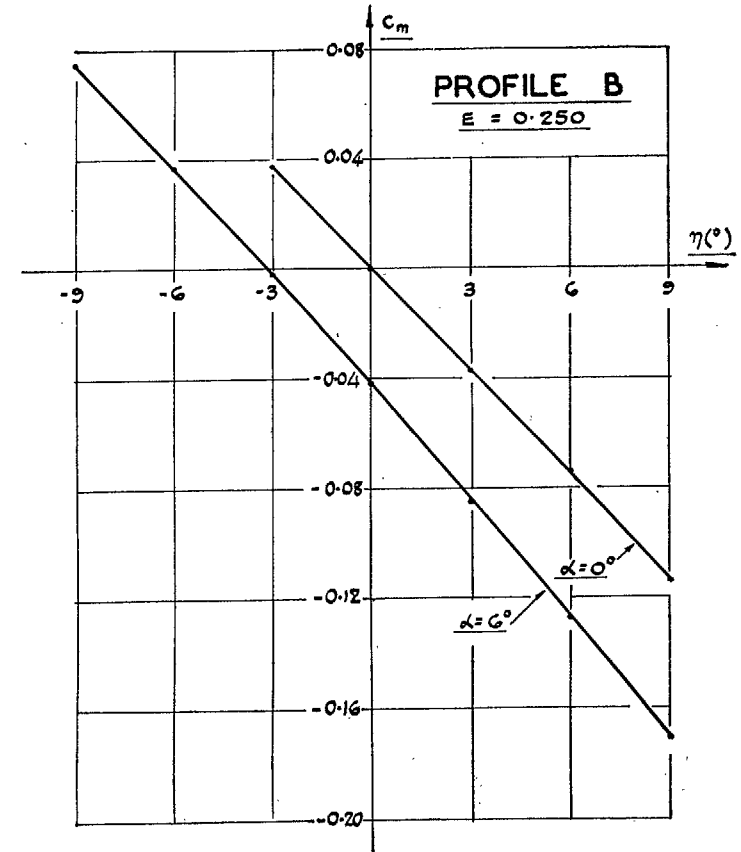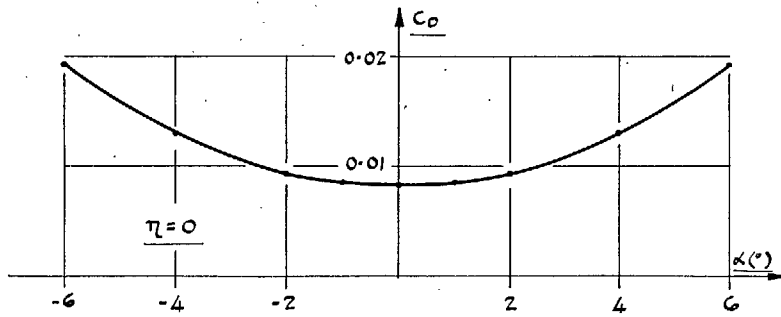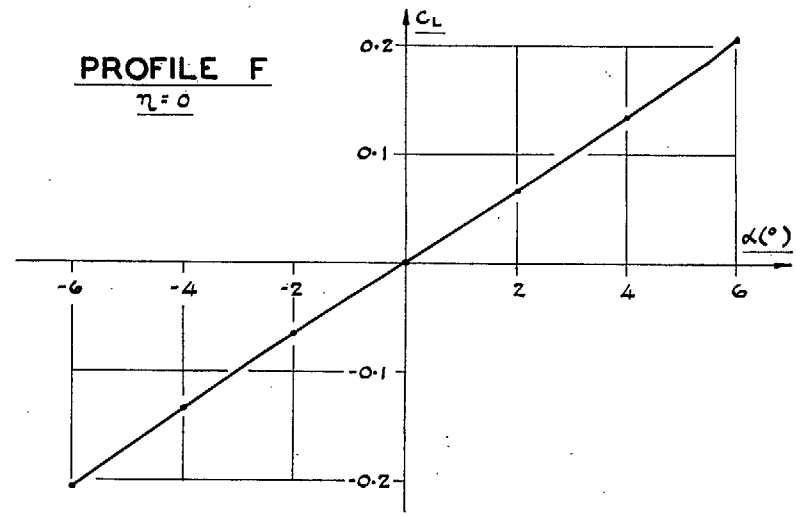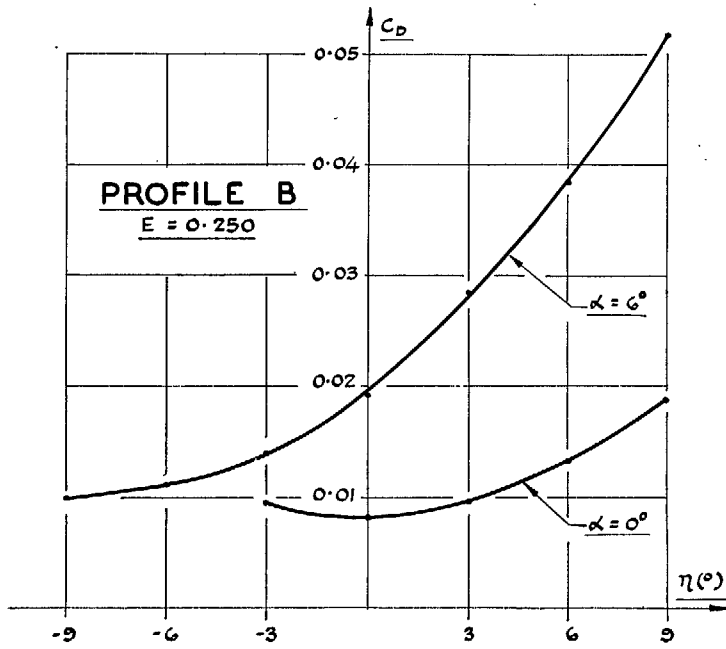
PROFILE B

$\eta = 0$

c_L

$\alpha(°)$

Fig. 6a.

c_m PROFILE B

$\eta = 0$

$\alpha(°)$

Fig. 7a.

c_L

PROFILE B

$E = 0.250$

$\alpha = 6°$

$\alpha = 0°$

$\eta(°)$

Fig. 6b.

c_m

PROFILE B

$E = 0.250$

$\eta(°)$

$\alpha = 0°$

$\alpha = 6°$

Fig. 7b.

FIG. 8a.

FIG. 9a.

FIG. 8b.

FIG. 9b.

17

FIG. 10a.

FIG. 11a.

FIG. 10b.

FIG. 11b.

Δ (PER RADIAN)   Re = 6 X 10^6

(AFTER COLLINGBOURNE)

1·5

1·0

0·5

E (DEGREES)

5   10   15   20   25

FIG. 12a.

$\dfrac{\Delta\,(6\times10^6)}{\Delta}$

(AFTER COLLINGBOURNE)

1·0

0·5

LOG₁₀ Re

6·0   6·2   6·4   6·6   6·8   7·0

FIG. 12b.

19

FIG. 13.

FIG. 14.

FOR FLAT WINGS OF RECTANGULAR PLANFORM

FIG. 15.

FIG. 16.

PROFILE A

$\alpha = 0, 1°, 2°, 4°, 6°$
$\eta = 0$

$\times$ $E = 0.250$ $\alpha = 0°, 6°$
$\eta = \pm 3°, \pm 6°, \pm 9°$

$C_D = C_{DO} + \dfrac{C_L^2}{\pi A}$

C_D

0.05

0.04

0.03

0.02

0.01

0.05   0.10   0.15   0.20 C_L^2

FIG. 17a.

22

FIG. 17b.

PROFILE C

$$C_D = C_{D0} + \frac{C_L^2}{\pi A}$$

FIG. 17c.

PROFILE D

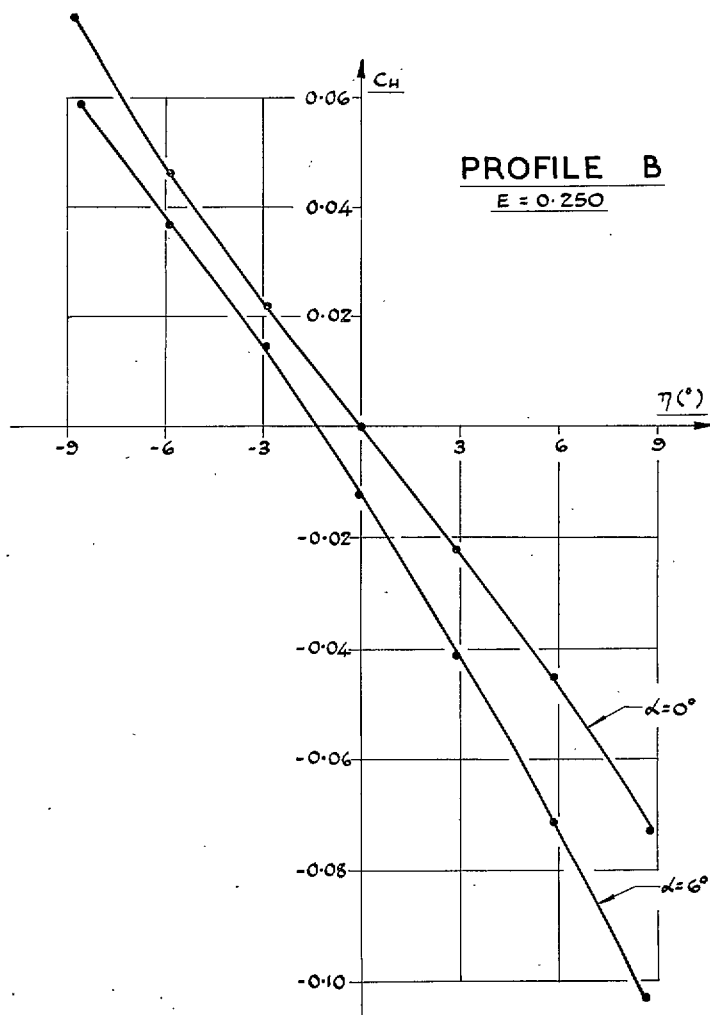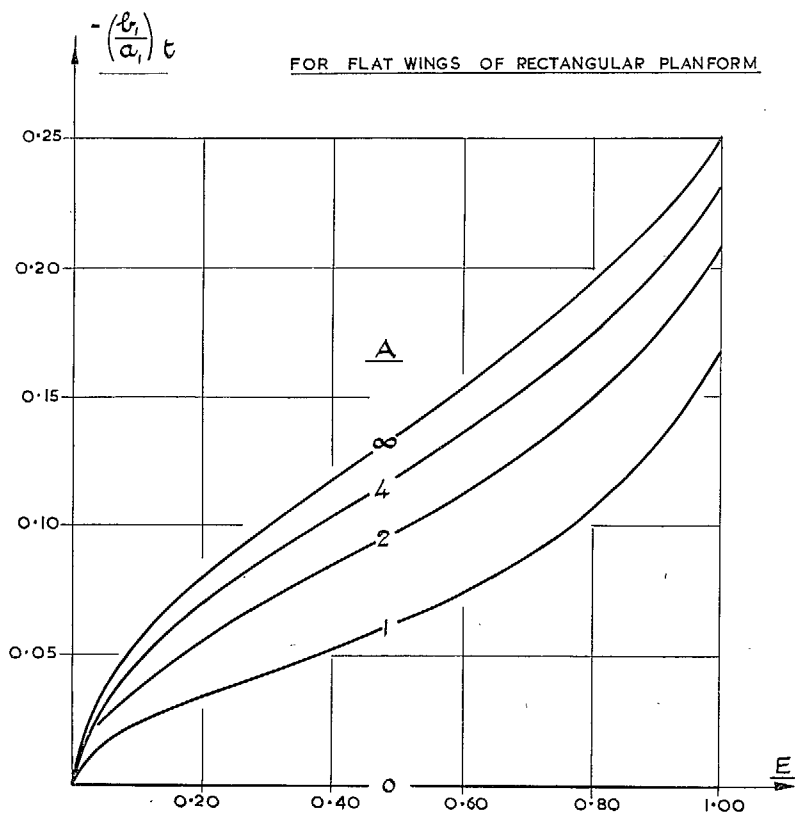$$C_D = C_{D0} + \frac{C_L^2}{\pi A}$$

FIG. 17d.

24
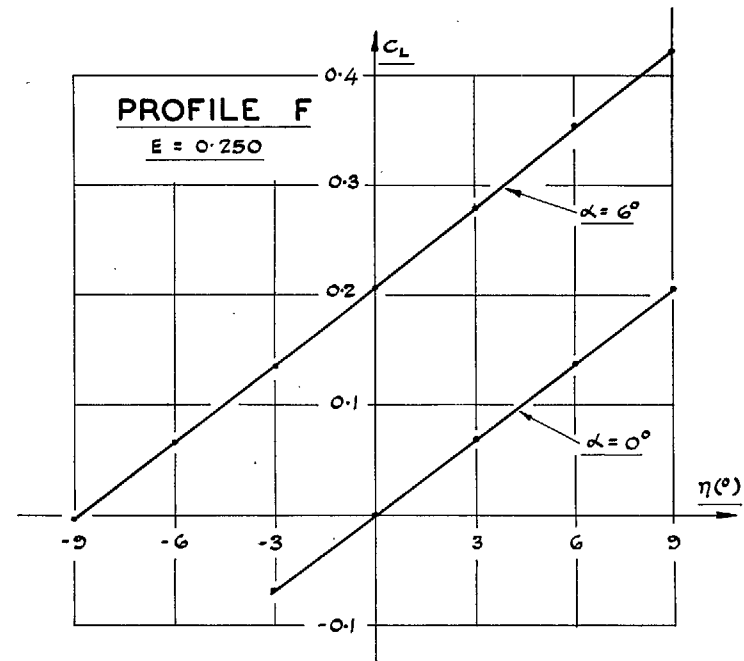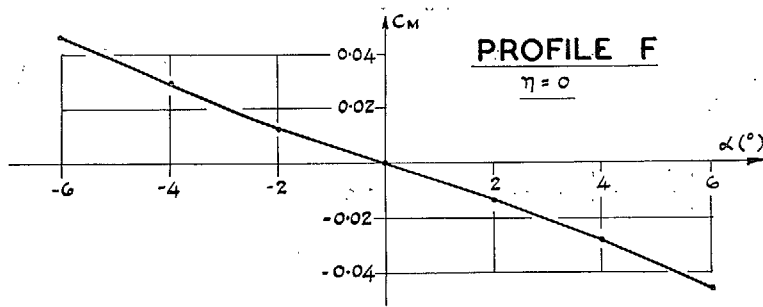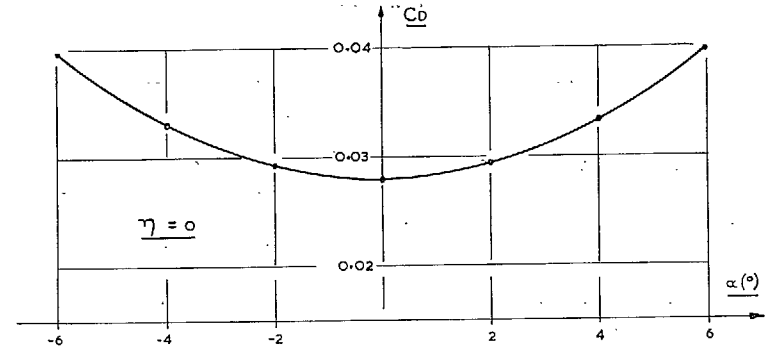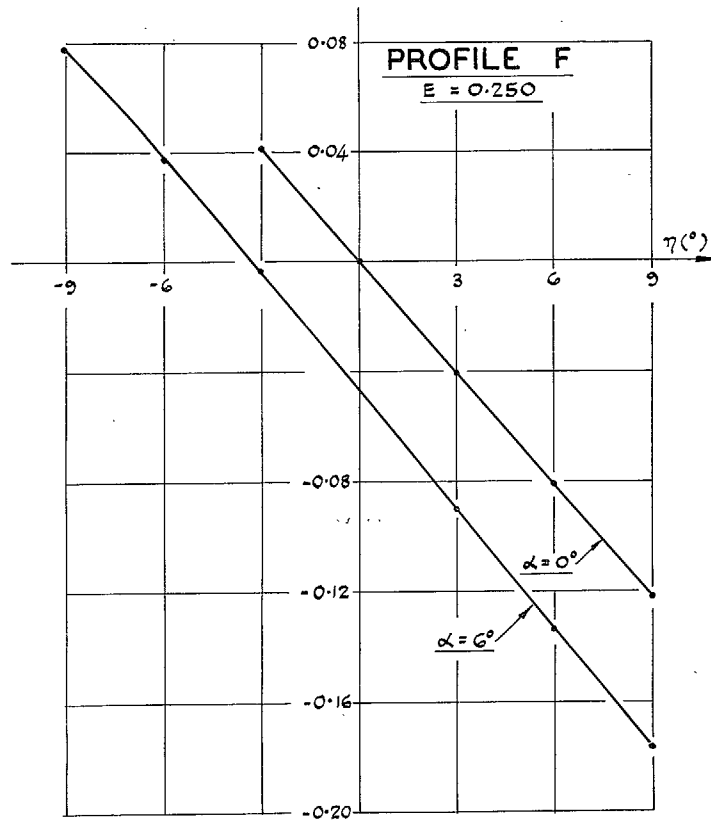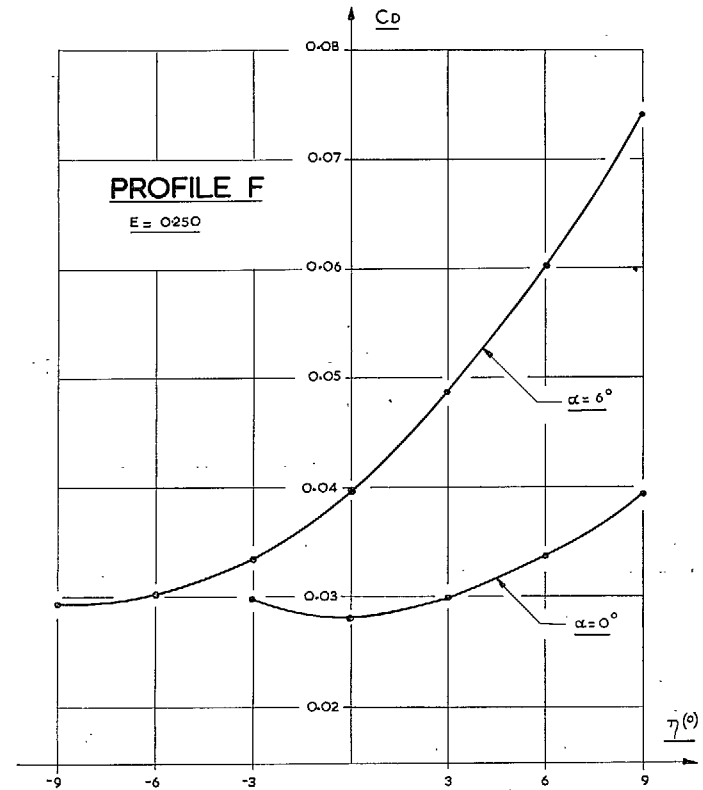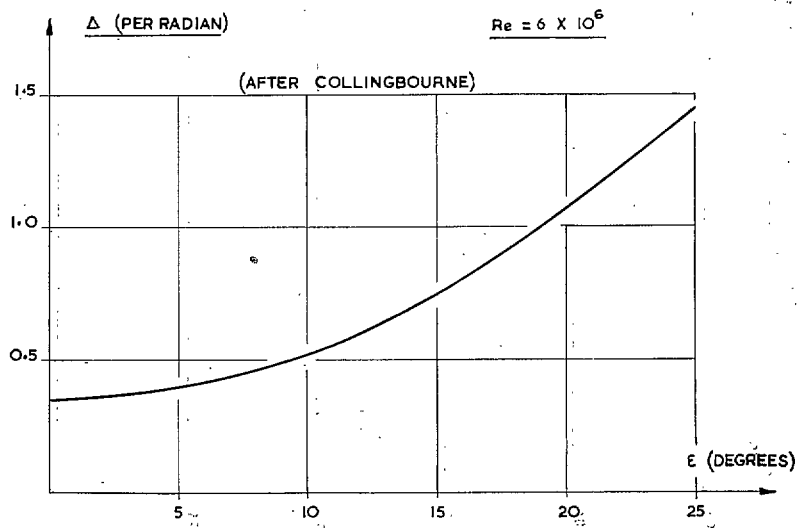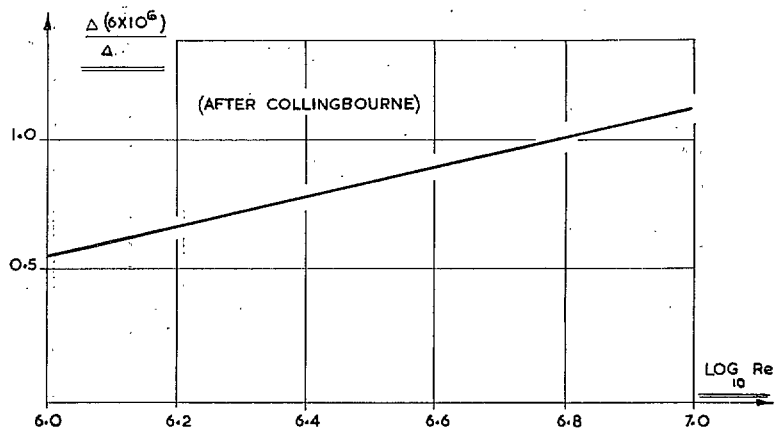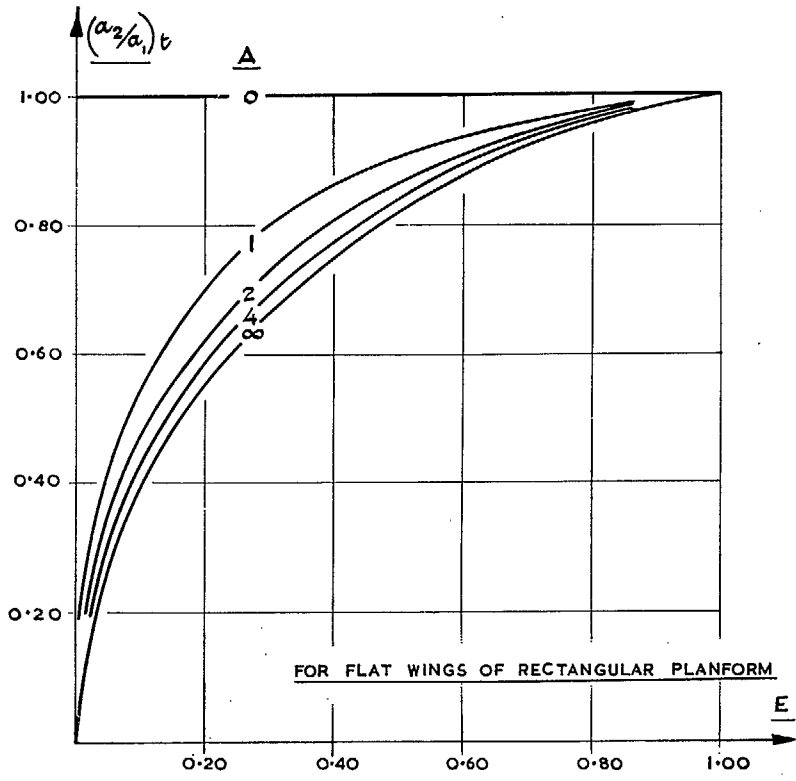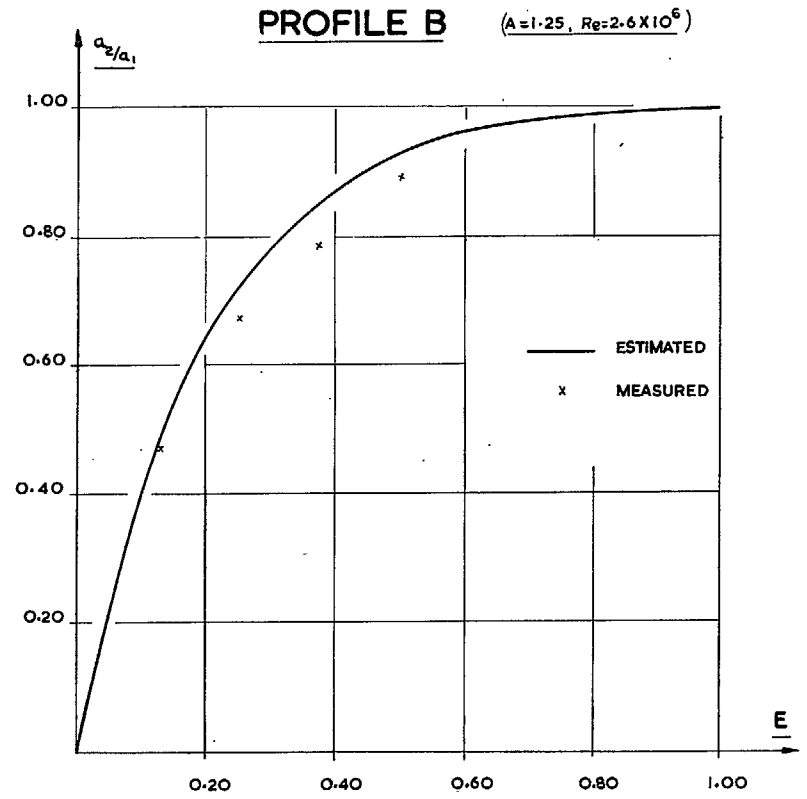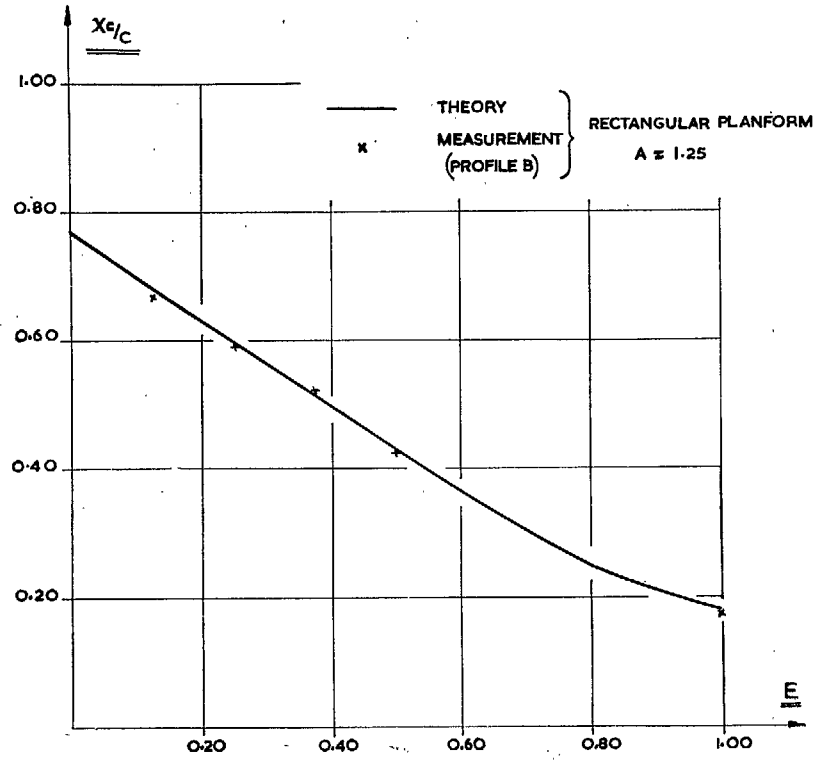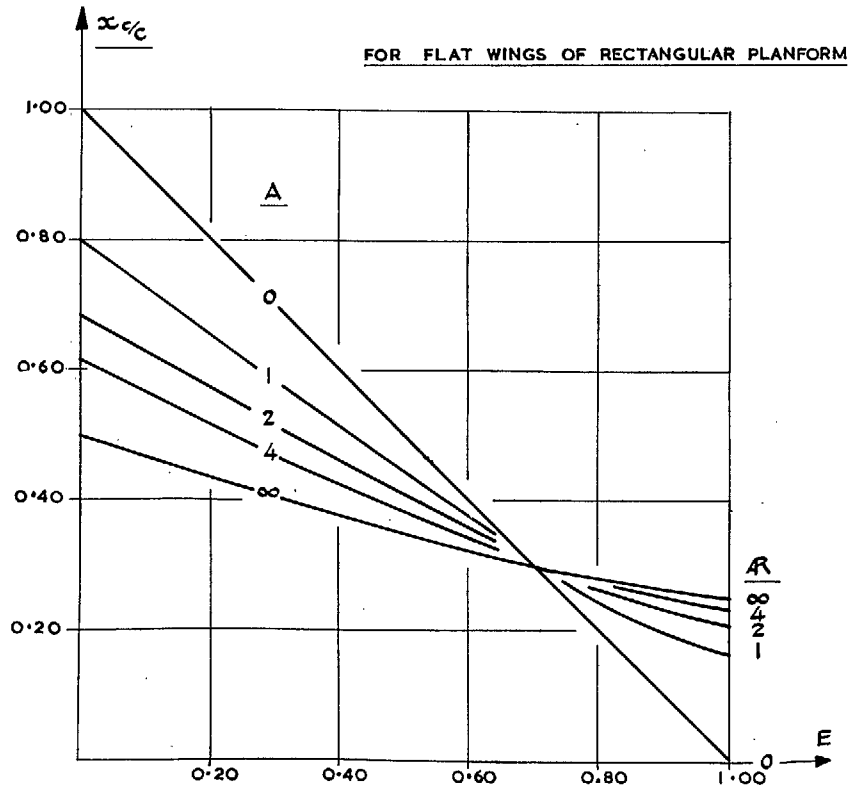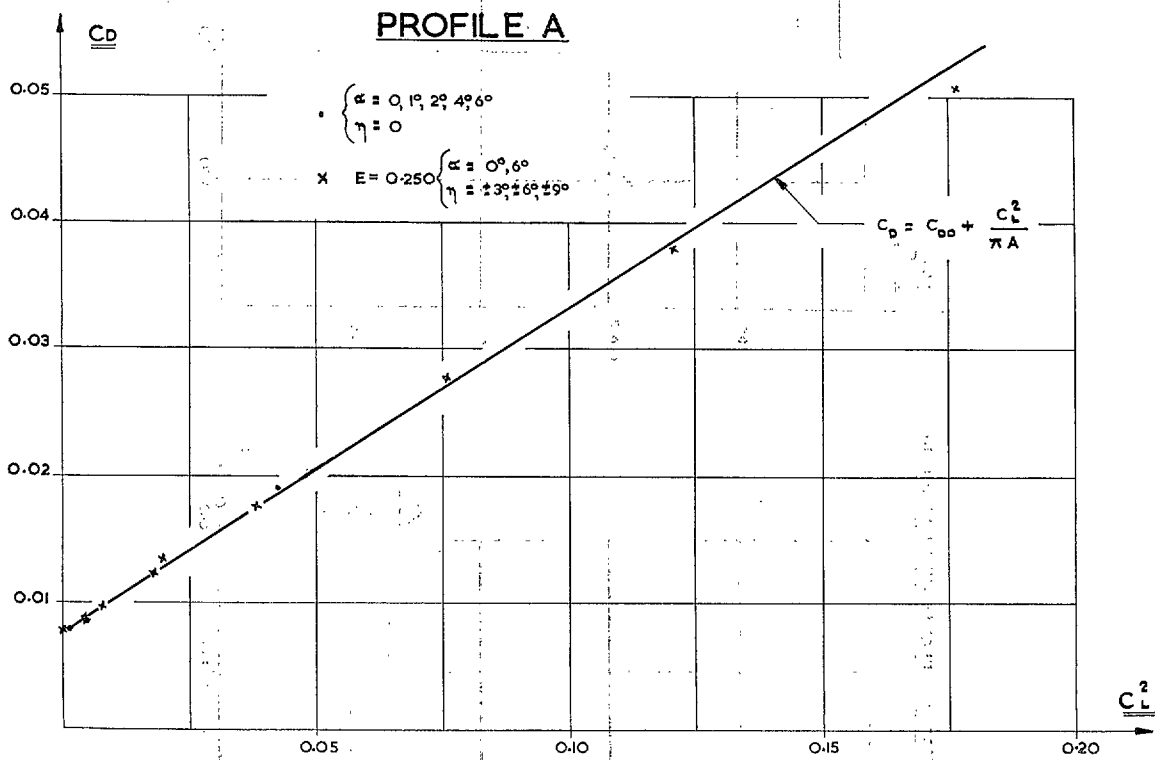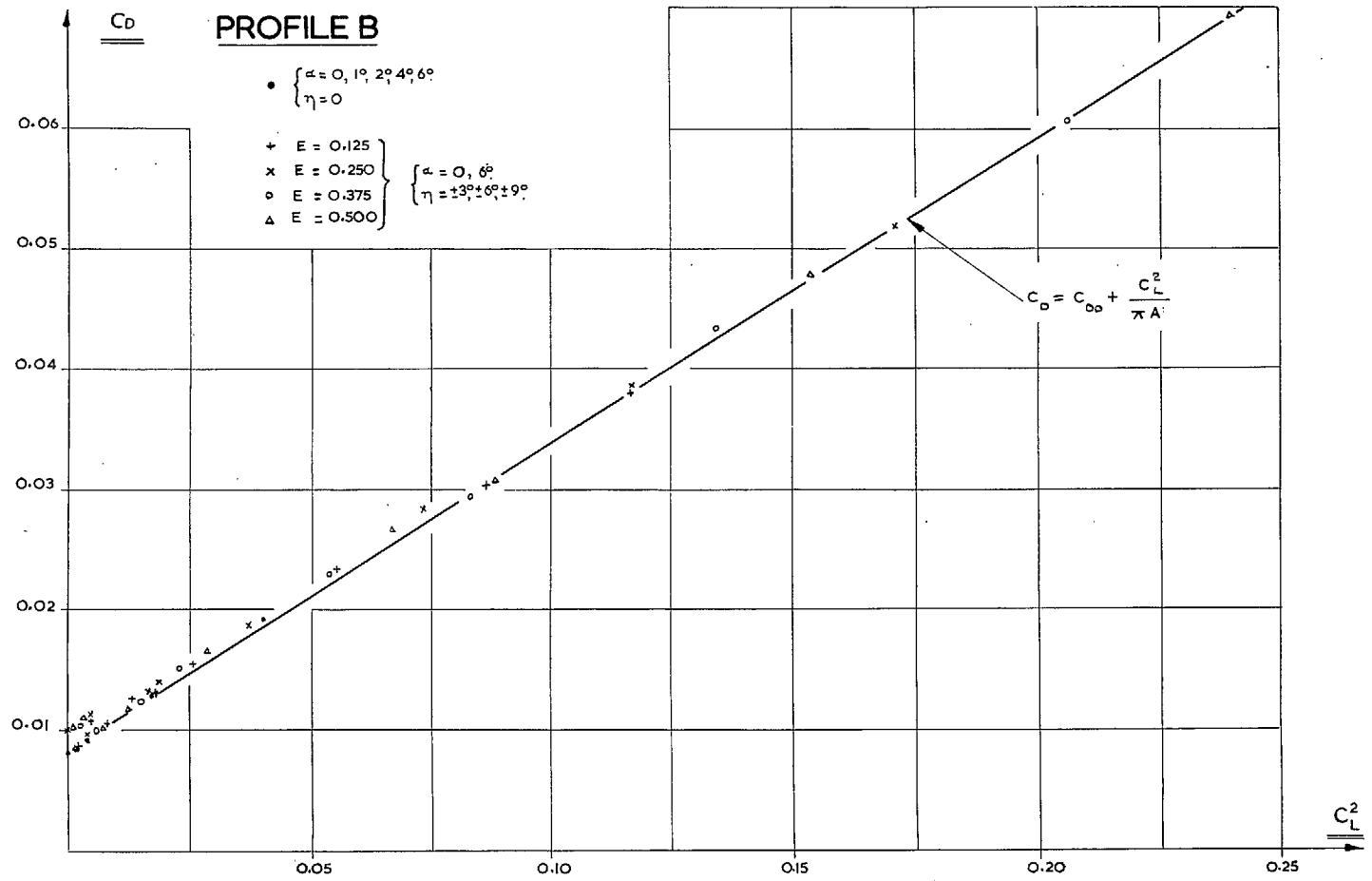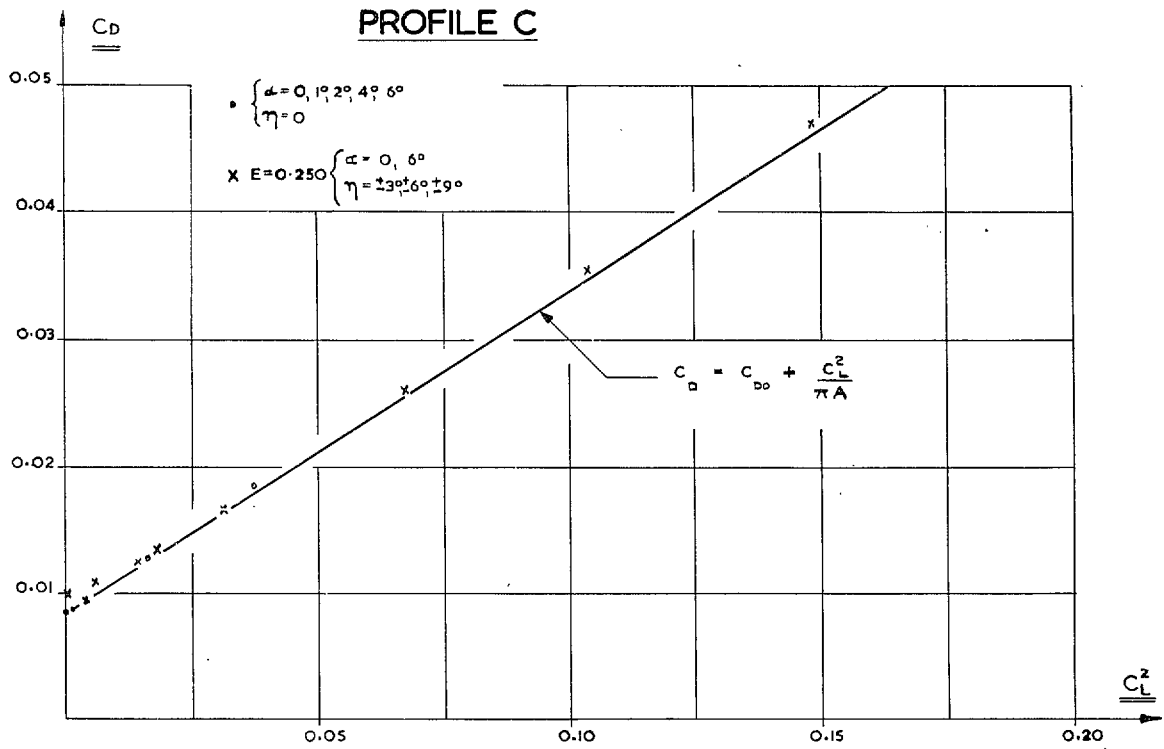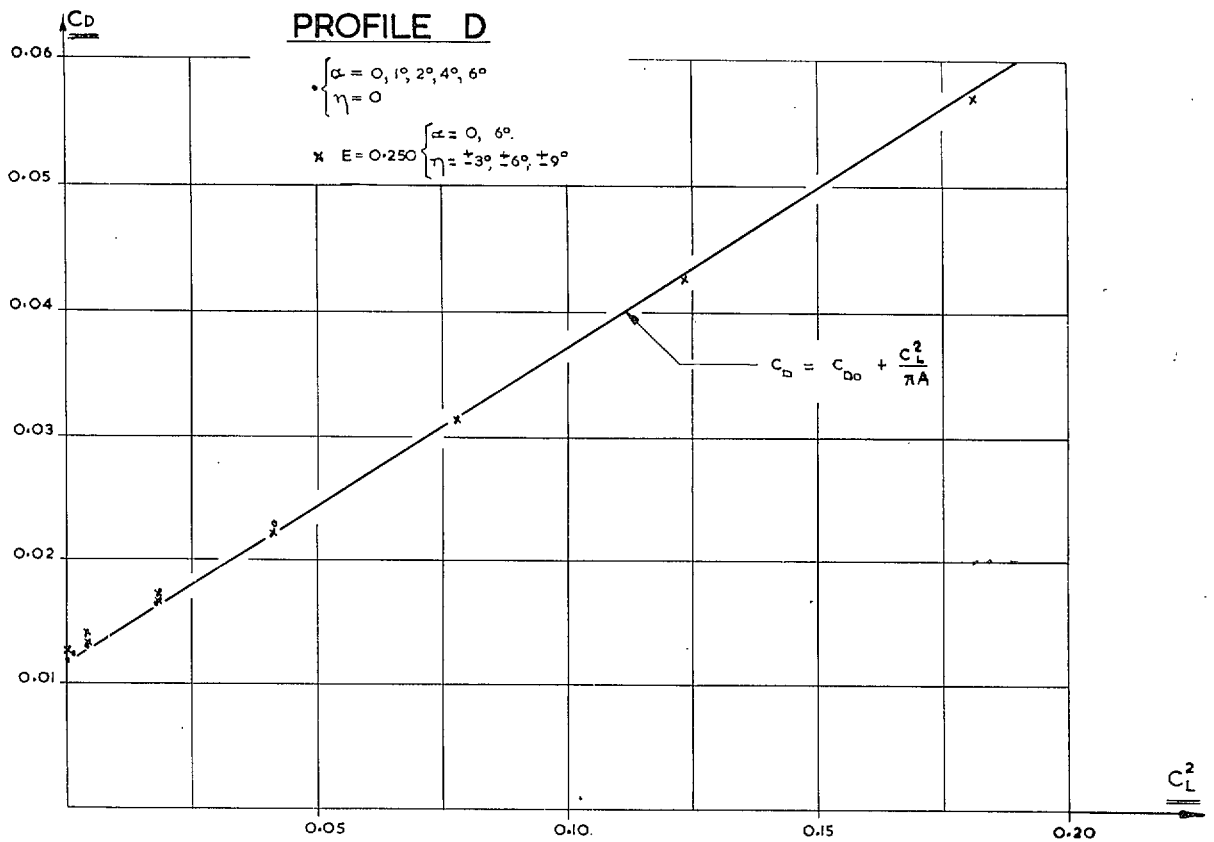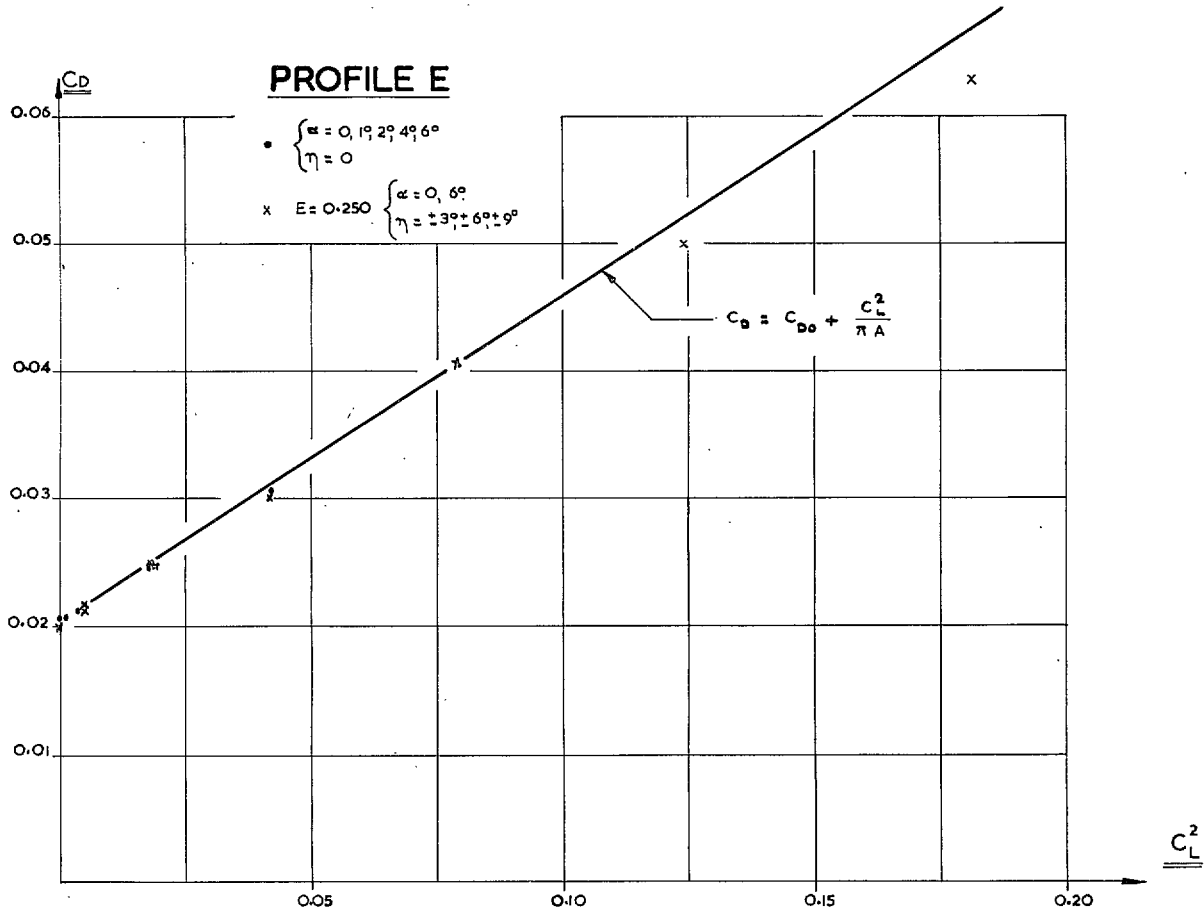
FIG. 17e.

FIG. 17f.

FIG. 18a.

FIG. 18b.

27

FOR FLAT WINGS OF RECTANGULAR PLANFORM

$-\left(\dfrac{\ell_{r_i}}{a_i}\right)t$

A

∞
4
2
1

$\dfrac{E}{A}$

FIG. 19.

FOR FLAT WINGS OF RECTANGULAR PLANFORM

$-\ell_t$

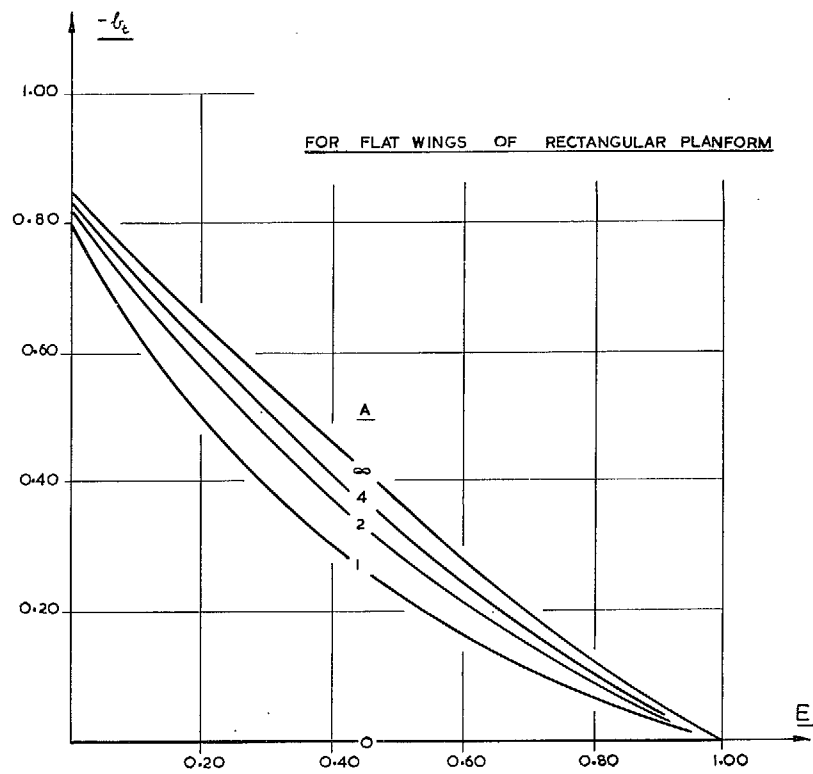A

∞
4
2
1

$\dfrac{E}{A}$
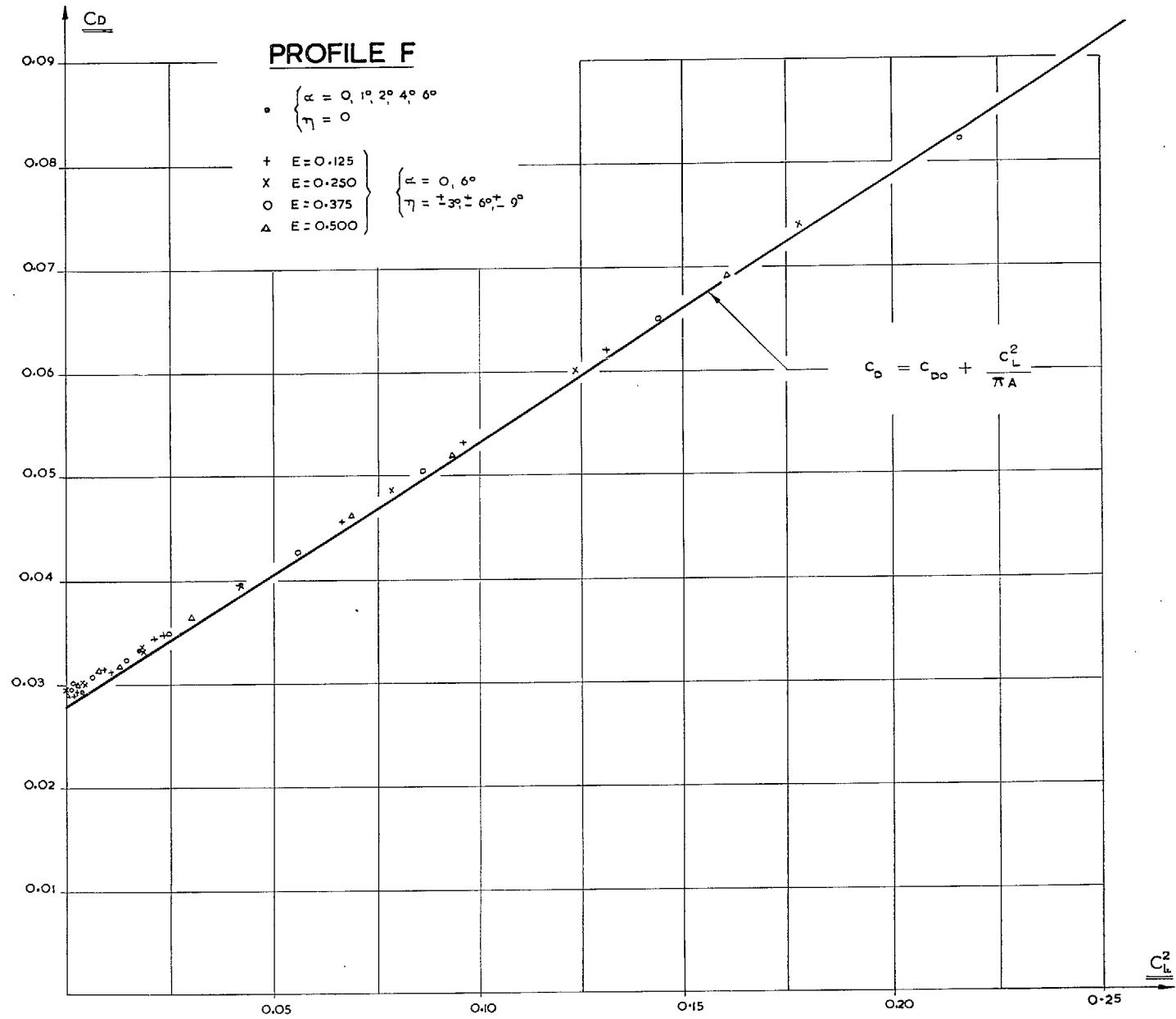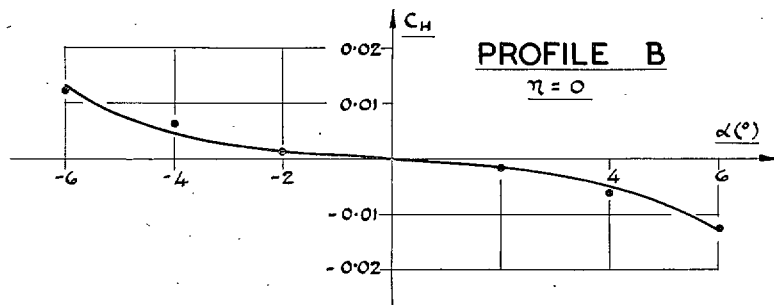
FIG. 20.

Publications of the
Aeronautical Research Council

ANNUAL TECHNICAL REPORTS OF THE AERONAUTICAL RESEARCH COUNCIL (BOUND VOLUMES)

1939 Vol. I. Aerodynamics General, Performance, Airscrews, Engines. 50s. (52s.).
   Vol. II. Stability and Control, Flutter and Vibration, Instruments, Structures, Seaplanes, etc. 63s. (65s.)

1940 Aero and Hydrodynamics, Aerofoils, Airscrews, Engines, Flutter, Icing, Stability and Control, Structures, and a miscellaneous section. 50s. (52s.)

1941 Aero and Hydrodynamics, Aerofoils, Airscrews, Engines, Flutter, Stability and Control, Structures. 63s. (65s.)

1942 Vol. I. Aero and Hydrodynamics, Aerofoils, Airscrews, Engines. 75s. (77s.)
   Vol. II. Noise, Parachutes, Stability and Control, Structures, Vibration, Wind Tunnels. 47s. 6d. (49s. 6d.)

1943 Vol. I. Aerodynamics, Aerofoils, Airscrews. 80s. (82s.)
   Vol. II. Engines, Flutter, Materials, Parachutes, Performance, Stability and Control, Structures. 90s. (92s. 9d.)

1944 Vol. I. Aero and Hydrodynamics, Aerofoils, Aircraft, Airscrews, Controls. 84s. (86s. 6d.)
   Vol. II. Flutter and Vibration, Materials, Miscellaneous, Navigation, Parachutes, Performance, Plates and Panels, Stability, Structures, Test Equipment, Wind Tunnels. 84s. (86s. 6d.)

1945 Vol. I. Aero and Hydrodynamics, Aerofoils. 130s. (132s. 9d.)
   Vol. II. Aircraft, Airscrews, Controls. 130s. (132s. 9d.)
   Vol. III. Flutter and Vibration, Instruments, Miscellaneous, Parachutes, Plates and Panels, Propulsion. 130s. (132s. 6d.)
   Vol. IV. Stability, Structures, Wind Tunnels, Wind Tunnel Technique. 130s. (132s. 6d.)

Annual Reports of the Aeronautical Research Council—

   1937 2s. (2s. 2d.)   1938 1s. 6d. (1s. 8d.)   1939–48 3s. (3s. 5d.)

Index to all Reports and Memoranda published in the Annual Technical Reports, and separately—

   April, 1950 -   -   -   -   R. & M. 2600 2s. 6d. (2s. 10d.)

Author Index to all Reports and Memoranda of the Aeronautical Research Council—

   1909—January, 1954   R. & M. No. 2570 15s. (15s. 8d.)

Indexes to the Technical Reports of the Aeronautical Research Council—

December 1, 1936—June 30, 1939	R. & M. No. 1850	1s. 3d. (1s. 5d.)
July 1, 1939—June 30, 1945	R. & M. No. 1950	1s. (1s. 2d.)
July 1, 1945—June 30, 1946	R. & M. No. 2050	1s. (1s. 2d.)
July 1, 1946—December 31, 1946	R. & M. No. 2150	1s. 3d. (1s. 5d.)
January 1, 1947—June 30, 1947	R. & M. No. 2250	1s. 3d. (1s. 5d.)

Published Reports and Memoranda of the Aeronautical Research Council—

Between Nos. 2251–2349	R. & M. No. 2350	1s. 9d. (1s. 11d.)
Between Nos. 2351–2449	R. & M. No. 2450	2s. (2s. 2d.)
Between Nos. 2451–2549	R. & M. No. 2550	2s. 6d. (2s. 10d.)
Between Nos. 2551–2649	R. & M. No. 2650	2s. 6d. (2s. 10d.)
Between Nos. 2651–2749	R. & M. No. 2750	2s. 6d. (2s. 10d.)

Prices in brackets include postage